ACS ENVIRONMENTAL Au
AN OPEN ACCESS JOURNAL OF THE AMERICAN CHEMICAL SOCIETY

Open Access
This article is licensed under CC-BY-NC-ND 4.0

pubs.acs.org/environau Review

Graphene Membrane for Water-Related Environmental Application: A Comprehensive Review and Perspectives

Published as part of ACS Environmental Au special issue "2024 Rising Stars in Environmental Research".

Junhyeok Kang,[§] Ohchan Kwon,[§] Jeong Pil Kim, Ju Yeon Kim, Jiwon Kim, Yonghwi Cho, and Dae Woo Kim*

Cite This: *ACS Environ. Au* 2025, 5, 35−60 Read Online

ACCESS | Metrics & More | Article Recommendations

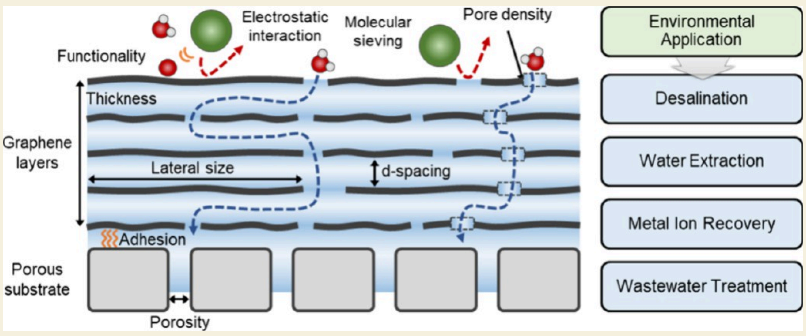

ABSTRACT: Graphene-based materials can be potentially utilized for separation membranes due to their unique structural properties such as precise molecular sieving by interlayer spacing or pore structure and excellent stability in harsh environmental conditions. Therefore, graphene-based membranes have been extensively demonstrated for various water treatment applications, including desalination, water extraction, and rare metal ion recovery. While most of the utilization has still been limited to the laboratory scale, emerging studies have dealt with scalable approaches to show commercial feasibility. This review summarizes the recent studies on diverse graphene membrane fabrications and their environmental applications related to water-containing conditions in addition to the molecular separation mechanism and critical factors related to graphene membrane performance. Additionally, we discuss future perspectives and challenges to provide insights into the practical applications of graphene-based membranes on the industrial scale.

KEYWORDS: *Graphene, Graphene oxide, Water treatment, Membrane, Resource recovery, Scalability, Module, Stability*

1. INTRODUCTION

Clean water scarcity has traditionally been crucial due to climate change, population growth, and urbanization; moreover, ultrapure water has been highly demanded owing to explosive development in high-value-added industries such as semiconductors, pharmaceuticals, hydrogen production, and batteries.[1−6] Therefore, numerous water treatment systems have been extensively reported and membrane separation is one of the promising technologies for water treatment due to its advantages of high energy efficiency, low operational cost, and being an integrated system.[7−9] Polymeric materials are commonly used for water treatment membranes due to their processability and cost-effectiveness. However, they normally face challenges such as low solvent permeance and stability issues during long-term operations.[10] To achieve better membrane performance, materials such as two-dimensional (2D) materials (graphene, MXene, transition metal dichalcogenides), metal−organic frameworks (MOFs), and covalent-organic frameworks (COFs) have been explored for membrane fabrication and used for various separations including gas separation, organic solvent treatment, and water treatment.[11−16]

Among those 2D materials, graphene and its derivatives are more optimized for solvent treatment membranes due to easy structure modification, excellent mechanical properties, and chemical resistance. Their relatively large nanochannels (surface pores and interlayer spacing) are suitable for separating ions and organic pollutants with subnanometer

Received: August 26, 2024
Revised: October 9, 2024
Accepted: October 9, 2024
Published: October 16, 2024

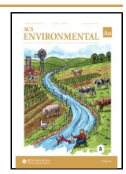

ACS Publications
© 2024 The Authors. Published by American Chemical Society

https://doi.org/10.1021/acsenvironau.4c00088
ACS Environ. Au 2025, 5, 35−60

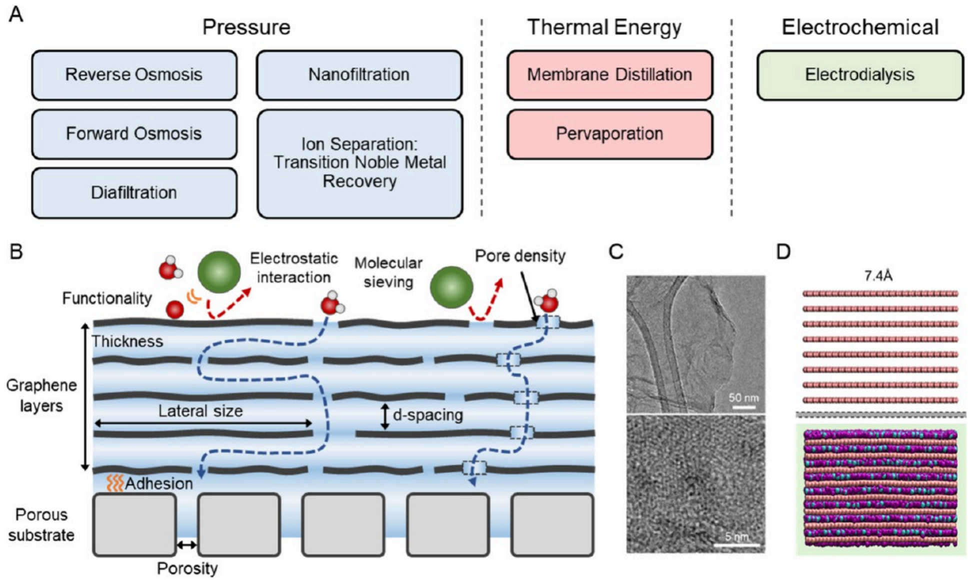

Figure 1. (A) Water-related membrane applications tested with graphene-based membranes according to their driving force for molecular transport. (B) Water transport and separation mechanism of a generalized laminated graphene membrane with critical factors governing membrane performances. (C) Low and high magnification TEM images of a graphene oxide nanosheet. Reprinted with permission from ref 57. Copyright 2023 Elsevier. (D) Water layer structure in a laminated graphene membrane with a *d*-spacing of 7.4 Å. Reprinted with permission under a creative commons CC BY 4.0 from ref 37. Copyright 2023 Springer Nature.

sizes.[17−19] Moreover, graphene derivatives can be synthesized in bulk scale via both dry and wet synthesis, which has been well established during the past few decades.[20] Therefore, graphene-based membranes have conventionally been utilized in various water treatment applications including desalination, organic pollutant removal, and water extraction. In addition, their use has recently expanded into resource recovery fields, including rare/noble metal ion recovery, which has extensively been demonstrated in lab-scale settings.[21−25] Further, research on graphene membranes has recently focused on developing scalable fabrication approaches to demonstrate their feasibility.[26−29] However, despite these advancements, the practical applications of graphene membranes on the industrial scale still face challenges, such as long-term stability issues, concentration polarization, and fouling; most importantly, graphene membranes have yet to be successfully applied in existing module systems, which remains a critical hurdle to their widespread adoption.

In this paper, we aim to provide a comprehensive overview of advances in graphene-based membranes, focusing specifically on water treatment technologies. Although many review papers have been reported on the fabrication of graphene-based membranes for water treatment, this review focuses more on the critical factors and aspects of the operation process and commercialization.[30−32] Therefore, the water transport and molecular sieving mechanisms on graphene membranes are elaborated at the beginning. In addition, various fabrication methods for graphene membranes are introduced, including both traditional and state-of-the-art techniques. Furthermore, research has explored various applications of graphene-based membranes in water treatment fields to demonstrate their development trend. Specifically, this review emphasizes diverse environmental applications including traditional desalination and emerging issues of resource (e.g., rare metal ions) recovery. At the end of this review, we discuss the prerequisites for practical application.

2. TYPES OF GRAPHENE MEMBRANES AND PREPARATION METHODS

2.1. Molecular Transport through Graphene-Based Membrane

The versatility of graphene derivatives allows for a variety of strategic modulations, tailored to the specific needs of the separation process, and the resulting membranes can be adopted in various applications regardless of their driving force (Figure 1A). These membranes are generally obtained in stacked superstructures which naturally arise from the 2D morphology of the sheets. Therefore, the overall trend of the graphene membrane is following the operation procedure of previous membranes such as polymer and ceramics, while there are growing efforts to find new applications that can maximize the potential of graphene materials.

As seen in Figure 1B, tuning the degree of oxidation, density of surface functional groups, aspect ratio, and porosity dictates the overall permeance and selectivity of the resulting membrane. Generally, graphene derivatives are loosely categorized into subgroups based on their synthetic history and chemical structures. Thus, graphene oxide (GO) and reduced graphene oxide (rGO) encompass a spectrum of materials with different functionalities and morphologies. The inherent imprecision of the terminologies can be deceptive, suggesting a universal chemistry among their constituents. However, the complex nature of graphene derivatives often prevents the consistency assumption underlying mechanism, and the transport through the membranes can significantly differ based on the morphology of the individual sheets as well as their overall structure. Therefore, proper characterization of the graphene sheets is critical for understanding and estimating overall membrane properties. In the scope of water permeation through laminated GO sheets, the dominant transport pathway consists of the 2D capillary network formed between the basal planes and the edges of the laminates.[33,34] Figure 1C shows the typical structure of GO. While the GO layer can be exfoliated into a single layer, the structure of its laminates can be highly influenced by the degree of oxidation and functional groups. Particularly, the *d*-spacing calculated from X-ray diffraction (XRD) measurements indicates the interlayer distances of GO stackings and serves as a key variable for tuning the membrane permeance and selectivity.[35,36] Dry GO laminates exhibit *d*-spacings around 0.8 nm, which is significantly larger than that of graphene sheets (0.34 nm) due to the decorated oxygen-containing groups on the basal plane. However, the interlayer distances of GO flakes are dynamic and sensitive to the permeating species and applied pressure. For water permeation, the *d*-spacing of GO membranes without any cross-linking effects can swell even up to 6−7 nm after long exposure to water and can be dispersed again in solvents, degrading molecular separation properties for small molecules and ions.[35]

Kang et al. presented simulated results with varyingly spaced graphene slits with respect to differing solvent permeations (Figure 1D).[37] It was calculated that slits with *d*-spacing above 7.4 Å allow the facile transfer of water as well as toluene, while ethanol transport requires larger slits of 8.4 Å. This result indicates that a minimum spacing is required for allowing solvent transport through the graphene layer. Therefore, the generation of oxygen-containing groups and defective structures is essential to induce fast solvent flow. Because highly oxidized GO is commonly used for membrane fabrication, the functional group reduction process leads to the restriction of the *d*-spacing of the sheets, while the selectivity and the membrane stability under solvents can be enhanced. The reduction of the GO sheets can limit the *d*-spacing to around 0.4 nm and this can be further tuned to specific targets with varying reduction methods including thermal, chemical, and electrochemical treatments.[37−40] While the value of *d*-spacing is critical, the alignment of the nanosheets is also critical, particularly for ion separation, commonly reporting high ion rejection rates with highly aligned graphene layers.

Individual GO sheets consist of hydrophobic sp^2 and functionalized sp^3 domains with perturbing oxygen-containing groups. Generally, streamlined transport occurs across the hydrophobic domains of the basal plane, whereas increased interactions (hydrogen bonding and electrostatic) within the sp^3 domains hinder the mobility of water molecules.[33] However, the functional groups also promote swelling and maintain the spaces between the laminates, which enhances the transport phenomenon.[41−43] Hence, the density and nature of the functional groups play key roles in membrane flux. Yu et al. prepared GO membranes with differing dominant functional groups (COOH, OH, and COC).[42] The results indicated that transport was proportional to the *d*-spacing of the laminated structure, with flux in the order of COOH > OH > COC. The *d*-spacing in both the dry and wet states was proportional to the size of the functional groups. The fast water permeance of COOH-dominant GO membranes also can be attributed to the defect generation on the plane of graphene oxide, because the COOH groups are formed at higher oxidation degree.[44]

Separately, Qui et al. studied the influence of edge-terminated functional groups on permeance.[45] Their results, largely computational, employed a tightly stacked laminate model, allowing single-layer water molecule transport. The edge functional groups studied were COOH, OH, and H. The article indicates that COOH termination limits water transport due to steric hindrance arising from the bulkiness of the group. Faster permeance was observed with H and OH groups due to minimized steric hindrance, while the OH group uniquely exhibited a pulling effect by an increased interaction with water. Additionally, surface functionality also allows increased selectivity toward ion separation. Zhang et al. coated the GO membranes with both positively and negatively charged polymers.[46] The positively charged membranes rejected the AB_2 type salts with divalent cations whereas the negatively charged membranes rejected the A_2B with monovalent cations. These results indicated that permeation of salts is dominated by electrostatic interactions between the membrane and the high-valent salts. Using the positively charged polyethylenimine (PEI) coated GO membrane, the authors further extended the results to separate monovalent and divalent ions.

The ionic environment adds further complexity to the swelling behavior of the GO stackings. First, under alkaline conditions, the oxygen-containing groups (COOH, OH) can be negatively ionized by losing the H^+ ion.[47,48] Enhanced electrostatic repulsion forces further enlarge the *d*-spacing of the laminates, increasing the permeation. Conversely, under acidic conditions, the ionization of the groups is limited, resulting in a hindered transport. Additionally, the chemistry of the cation leads to certain cross-linking behaviors. Transition metal ions, including Mn^{2+}, Fe^{3+}, Cu^{2+}, and Cd^{2+}, coordinate with the functional groups through d-orbital-sp^3 interactions between the sheets, limiting swelling and permeation through the GO sheets.[49] Recently, Wen et al. revealed that for ion-intercalated GO membranes, the ions act as hydrophilic impurities.[50] Thus, water permeation is not related to the size of the ions (steric effect) but to the ion's affinity toward water molecules. Strongly interacting ions, such as Ca^{2+}, Mg^{2+}, and Fe^{3+}, which have larger hydrated diameters, impede water transport more significantly.

The 2D nature of graphene sheets implies that the longest permeation pathway is in-plane permeation through the basal planes of the laminated sheets. Additionally, through-plane permeation occurs through the edge capillaries. A higher density of interedge pathways can be controlled by decreasing the size of the individual sheets, which minimizes the tortuosity of the membranes and increases the overall flux. Nie et al. utilized an ultrasonic method to decrease the lateral dimensions of the GO sheets, resulting in flakes sized 0.03 μm^2. Untreated GO sheets were measured to be around 47 μm^2 wide with a wide distribution.[51] The GO membranes were stabilized with La^{3+} ions. For all tested permeating solvents, including water, the small-flaked membranes exhibited a higher permeance under equal conditions. Computational studies done by Muscatello et al. also suggest that the distance between the entrance and exit slits is a critical aspect in water permeance.[52] The results indicate that the lower the distance between the openings, the faster the permeance, which could indicate that the higher density of interedge pathways can result in increased water transport.

More recently, Kim et al. employed a similar methodology for preparing smaller-sized GO sheets which were further stabilized by thermal treatment.[53] The theoretical permeation pathway of the small-flake membranes was 2.5 times shorter. However, when tested for actual water transport behaviors, membranes composed of larger-flaked GO exhibited a 3.3 times higher permeance. This opposing phenomenon was attributed to the lower *d*-spacing and higher compaction of the smaller GO sheets. The contradictory results reported in the literature imply the difficulty in precise modulation of membrane properties, arising from the dependency of each

https://doi.org/10.1021/acsenvironau.4c00088
ACS Environ. Au 2025, 5, 35−60

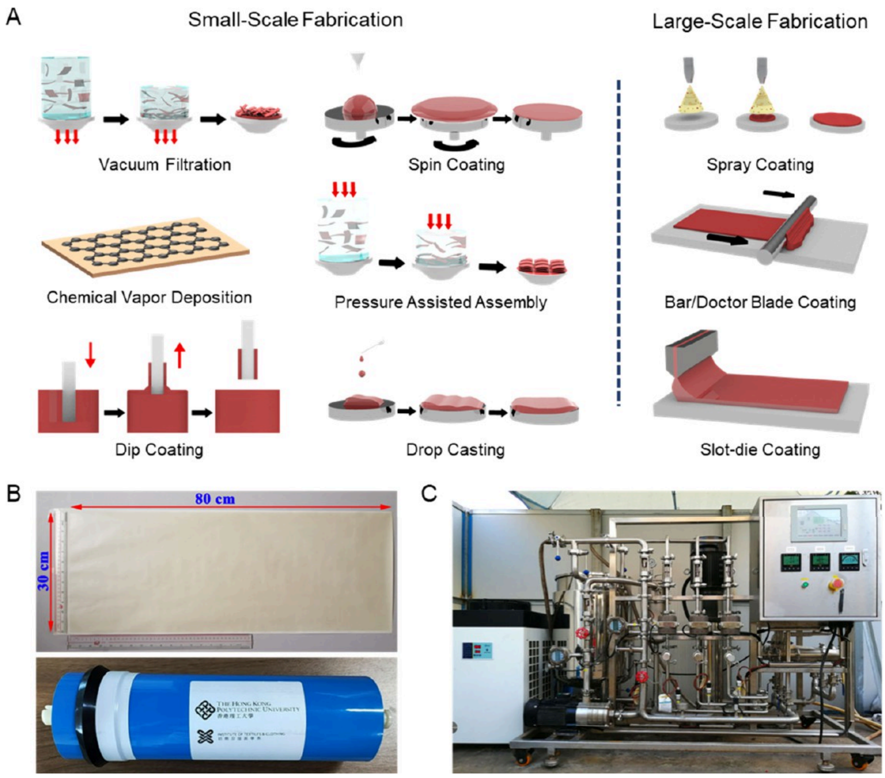

Figure 2. (A) Fabrication methods for preparing graphene-based membranes categorized by their scalability. Reproduced with permission under a creative commons CC BY 4.0 from ref 27. Copyright 2021 MDPI. (B) Large area fabrication of GO membranes by bar coating and its module, and (C) Pilot testing setup of the GO membrane. Reprinted with permission from ref 73. Copyright 2022 Elsevier.

Table 1. Summary of Graphene-Based Membrane Fabrication Methods

Scale	Advantage	Disadvantage	Scalability
Vacuum filtration	Simple and easy to control the membrane thickness	Limited to small areas	Low
Spin coating	Capable of producing uniform and ultrathin membranes	Limited to small areas and substrate with smooth surface	Low
CVD	Effective for producing high-quality graphene	High cost and complex equipment required	Low
Pressure assisted assembly	Effective for preparing dense and well-ordered thick layers	Limited to small areas	Low
Drop casting	Simple and cost-effective method	Limited to small areas and difficult for well-ordered layers	Very low
Dip coating	Simple coating process and insensitive to the shape of the substrate	Difficult for precise thickness control and uniformity	Moderate
Spray coating	Insensitive to the shape of the substrate	Difficult to prepare uniform film	High
Bar/doctor blade coating	Effective for preparing well-ordered layers	Sensitive to the shape of the substrate	High
Slot-die coating	Enable continuous coating method	Requires specialized equipment	Very high

physical property where one affects the other in a trade-off relationship. Hence, a holistic viewpoint must be imposed for controlling the characteristics of GO.

Another pathway for through-plane permeance within the stacked architecture is through defective pores existing on the basal planes. Generally, for scalable production of pores, thermal treatment or chemical etching methods are often employed. Lin et al. proposed the mechanism of pore development using thermal treatment, concluding that epoxy groups evolve as CO_2 during the reduction process, leaving defective pore sites.[54] By controlling the epoxy ratio, we can tune the size of the nanopores can be tuned. Xu et al. proposed the use of H_2O_2 as an etching reagent under heated conditions (100 °C), where sufficiently high concentrations were required to yield the pores.[55] Regardless of the method, perforation leads to enhanced through-plane transport of the materials.

Kim's group has widely adopted thermal treatment to yield nanoporous reduced graphene oxide (rGO) sheets for various membrane applications, including nanofiltration, gas separation, and ion separation.[25,37,56,57] Most notably, under cross-flow experiments for dye molecule separation, the nanoporous rGO membrane initially showed a water permeance of 131 L m^{-2} h^{-1} bar^{-1} compared to that of the GO membrane, which exhibited a permeance of 23 L m^{-2} h^{-1} bar^{-1}. Furthermore, after 22 h, the decrease in flux of the rGO membrane was 49%, whereas the decrease in the GO membrane was more severe at 71%. Several computational studies have been conducted to reveal water transport through an open pore in single-layer graphene sheets. Suk et al. indicated that the permeance of water molecules is faster in carbon nanotube (CNT) channels when a single-file structure is observed, which corresponds to 0.75 nm-sized pores.[58] In larger pore cases, the water transport

https://doi.org/10.1021/acsenvironau.4c00088
ACS Environ. Au 2025, 5, 35−60

in graphene membranes is higher due to the reduced energy required to enter the pores. Cohen-Tanugi et al. studied the effect of terminated functional groups on the edge of the pores.[59] The results highlighted that hydrophilic hydroxyl-terminated pores retain faster water permeance due to hydrogen bonding but concurrently reduce salt rejection, as the OH groups facilitate the passage of salt ions by lowering the energy barrier, thus creating a trade-off between water flux and salt rejection. Moreover, it is expected that the molecular separation of the laminated graphene membrane is governed by the interlayer spacing rather than nanopores when the size of the nanopores is larger than 1 nm. Therefore, the pores act as additional entrances rather than sieves, contributing to the enhancement of water permeation.[21]

2.2. Fabrication of Graphene-Based Membrane

GO is typically synthesized through the oxidation of graphite using methods like Hummers' method or its modifications. The process generally begins with the intercalation of graphite with strong oxidizing agents, such as a mixture of sulfuric acid and potassium permanganate.[60−62] This reaction introduces oxygen-containing groups (such as OH, COC, and COOH groups) into the graphite structure, resulting in exfoliation of the GO layers. The oxidation process is carefully controlled to balance the extent of oxidation and maintain the layered structure. GO is obtained in aqueous dispersions, which could be diluted or concentrated to fabricate film structures through various pathways. Common methods include vacuum filtration, spin-coating, dip-coating, and bar-coating (Figure 2A and Table 1). While much of the research has focused on employing small-scale methods, in the past decade, scalable fabrication methods have been sought due to their higher feasibility for industrial adoption. Here, the term "scalable" indicates that the process can be achieved in a continuous pathway rather than lab-scale batch productions.[27]

Most commonly, graphene-based membranes are produced by vacuum filtration of the dispersed solution. The laminates are deposited on a porous substrate, which increases the mechanical stability. Additionally, the stacked layer can be delaminated to yield free-standing films. The thickness of the membranes can be varied from nanometer scales to micrometer scales by controlling the concentration and the amount of the filtrated solution. Dikin et al. prepared freestanding GO papers through the vacuum filtration method, which were later expanded by Nair's group to test for ion permeation properties at high pressure conditions.[36,63] More recently, Kang et al. produced porous rGO membranes with high crystallinity, which were reduced by microwave irradiation.[37] The obtained tortuous rGO flakes were laminated with vacuum filtration. Interestingly, these membranes had dynamic cutoff properties based on the permeating solvent due to the different swelling of the stacked channels. Vacuum filtration method is particularly effective when the graphene exfoliation is hard to achieve and when graphene is soluble in a low concentration range. By removing the thick nanosheets by centrifugation, uniformly stacked graphene layers can be prepared via vacuum filtration, while large-scale fabrication is hard to achieve.

Similar to the vacuum filtration method, additional pressures can be applied to the filtrate side, increasing the force exerted on the membrane during deposition. The additional pressure aids in ordering of the laminate structure. Tsou et al. prepared GO membranes using different methods, including pressure-assisted filtration, vacuum filtration, and simple evaporation.[64] The results indicated that due to the higher degree of ordering, the membranes were thinner, and the hydrophilicity was enhanced by more exposed hydrophilic edge sites. Spin-coating is another widely adopted technique for the fabrication of thin films. For GO membranes, the centrifugal force applied during the coating process acts as a shear force, creating a laminated architecture. Additionally, spin-coating can be relatively precise, yielding thinner membranes on a scale of a few nanometers. Nair et al. successfully prepared membranes through spin or spray coating on Cu substrates, which were later selectively etched to yield 1 cm diameter membranes.[38] Shen et al. further demonstrated the spin-coating method with external pressures to yield a denser polymer-GO laminate membrane.[65] These membranes had a tightly ordered structure that could be used for H_2/CO_2 separation.

Generally, vacuum filtration or spin-coating methods require planar substrates, whereas dip-coating is a method that disregards the substrate shape. This straightforward process involves the substrate being submerged in a stock GO solution, which is later drawn out. Thus, the technique can be applied to various substrates, including hollow fiber membranes. The 2D sheet orientation can be modified by optimizing variables such as the solution viscosity and pulling rate. Zhang et al. demonstrated GO/Pebax hollow fiber membranes by the dip-coating method which exhibited CO_2/N_2 selectivity.[66] Eum et al. reported ethylenediamine (EDA) functionalized polyvinylidene fluoride (PVDF) hollow fiber membranes for nanofiltration. In this research, the GO layer was deposited on to the hollow fibers by the dip-coating method. Due to the spontaneous cross-linking reaction of the unreacted EDA with the GO, the selective layer can be formed relatively easily. However, the low permeance of the water indicates that further tuning of the GO layer and the substrate fiber is needed.[17]

The introduced techniques up to now have been focused on batch-scale processing, producing membranes in a non-continuous manner. However, given that membrane technology is inherently more relevant to industrial applications, the discussion must be expanded to scalable methods. Generally, methods such as bar-coating, doctor blade, or slot-die coating can be fitted into a roll-to-roll setup, facilitating the production rate. Aqueous GO dispersion can be concentrated into gel-like solutions that exhibit shear-thinning viscoelastic behavior. Additionally, GO concentrations can be lowered while maintaining viscosity using ionic liquids to balance electrostatic interactions, which can be beneficial for yielding thinner membranes. Thus, when a shear force is applied to the GO sheets through a bar or doctor blade, they can be aligned in a laminated architecture. Akbari et al. presented the scalable production of laminated GO membranes on nylon substrates using a gravure printing machine.[67] In this research, the GO solutions were first concentrated to form hydrogels (~40 mg/mL), and their rheology data indicated the development of shear-thinning behavior. Choi et al. coated GO hydrogels on porous nylon films using a bar coater, which was further cross-linked by EDA vapor exposure.[68] In another study, GO hydrogels were applied on poly(ether sulfone) support and reduced by applying external pressure and temperature.[25] During the hot-press step, the membrane maintained its highly ordered structure, while developing nanopores on the basal plane.

Conversely, the slot-die technique is more versatile and can be extended to employ relatively low concentration GO dispersions. While the installation cost can be higher than

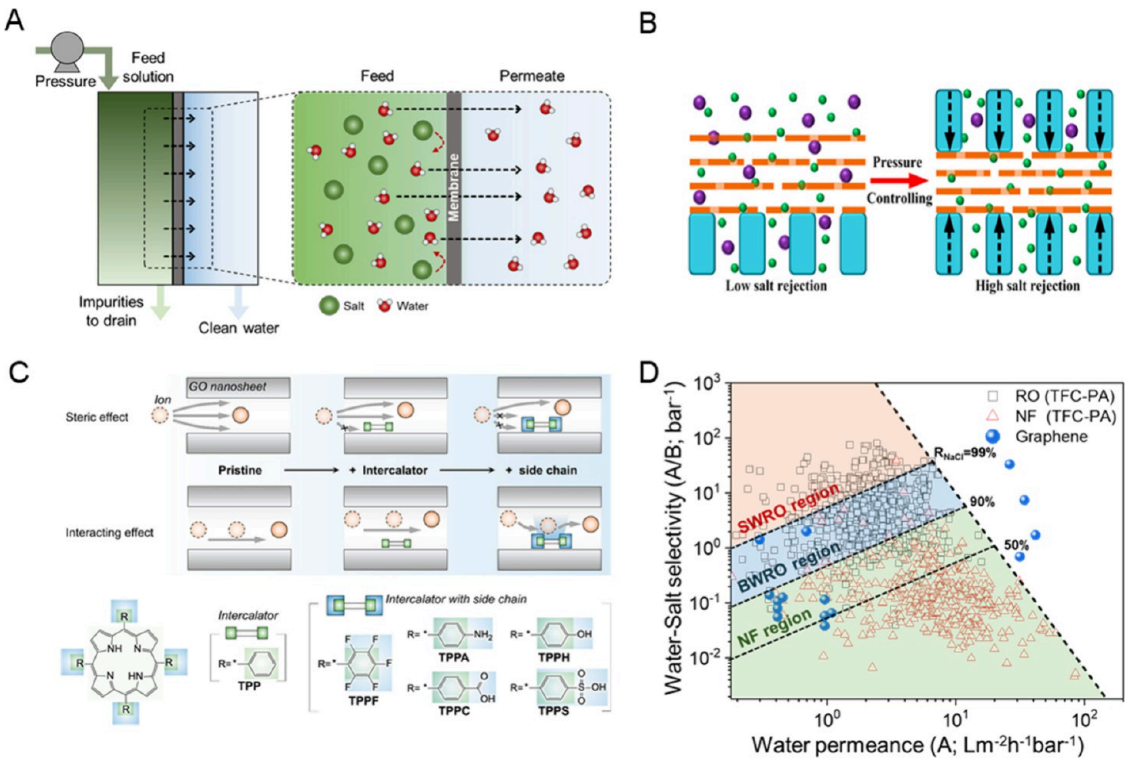

Figure 3. (A) Schematic of the reverse osmosis process. (B) Schematic of external pressure regulation phenomena of the graphene oxide membrane. Reprinted with permission from ref 81. Copyright 2018 American Chemical Society. (C) Illustrations for the effect of intercalants on the ion transport in the interlayer spacing of graphene nanosheets. Reprinted with permission from ref 83. Copyright 2023 American Chemical Society. (D) Comparison of desalination performances for thin-film composite polyamide (TFC-PA), and graphene-based membranes. The dashed lines indicate seawater reverse osmosis (SWRO; NaCl rejection > 99%), brackish water RO (BWRO; 90% < rejection < 99%), and nanofiltration (NF; rejection < 90%) regions. The values of water permeance (A) and salt permeability coefficient (B) for PA membranes were obtained from ref 90.

typical bar-coating, the major benefit is that the thickness of the membrane can be reduced, increasing the total permeance of the membrane. The GO solution is extruded through a slot-die head, where the initial shear force is applied. Additionally, the horizontally moving substrate under the meniscus further aligns the GO on the target substrate, producing a highly stacked laminate architecture even in relatively thin membranes (~100 nm scale).[69] Kim et al. prepared deoxygenated GO dispersions with a concentration of 20 mg/mL.[26] Using a slot-die coater, the membrane thickness can be controlled within the ~100 nm scale, with a 400 nm membrane being used for nanofiltration applications. Separately, in a follow-up study, the group successfully demonstrated sub-200 nm thick membranes using a slot-die coater in tandem with the hot-press method.[57] The slot-die coating is not only limited to graphene oxides, but also applicable to various 2D materials as demonstrated for MXene, TMDs, and graphene nanoribbons (GNRs).[70,71]

As shown in Figure 2B and C, for realistic adoption of GO membranes, the small-scale fabrication methods are insufficient in providing the necessary sizes of the membranes.[72,73] Xin et al. recently demonstrated pilot-scale GO-based dyehouse effluent separation. These membranes are prepared by the bar-coating method which resulted in membranes in the size of 2,400 cm^2 and were reduced by ultraviolet light irradiation. The optimized values of operation 32 °C, 5 bar with a flow rate of 0.25 m/s. Further considerations toward industrial adoption of membranes will be discussed in the perspective section.

3. WATER-RELATED APPLICATIONS OF GRAPHENE-BASED MEMBRANES

3.1. Reverse Osmosis

Reverse osmosis (RO) is one of the most widely utilized membrane separation technologies in the field of water treatment, in which water molecules move from a solution with a higher concentration to one with a lower concentration through a semipermeable membrane. In the RO process, external pressure is applied to overcome osmotic pressure, allowing water to pass through the membrane while effectively rejecting a wide range of contaminants such as salts, heavy metals, and organic compounds (Figure 3A). Therefore, RO membranes are commonly used in desalination, wastewater treatment, and potable water production.[74] The RO membranes are described as dense nonporous membranes (pore size < 1 nm), which are typically polymeric, mainly thin-film composite (TFC) polyamide (PA) membranes.[75,76] The PA membranes achieved a breakthrough in salt separation applications nearly half a century ago; however, they still suffer from extremely low water permeance (up to 3 L m^{-2} h^{-1} bar^{-1}) and low chlorine resistance.[76,77] Here, high chlorine ion concentration occurs during the desalination processes, including salt concentration and membrane cleaning, possibly leading to chemical degradation of the membranes, severe scaling, and decreased membrane lifespan and performance. Additionally, the fabrication of PA membranes often requires the use of harmful organic solvents such as *n*-hexane or toluene, raising environmental and safety concerns.[78,79]

https://doi.org/10.1021/acsenvironau.4c00088
ACS Environ. Au 2025, 5, 35−60

Table 2. Summary of Desalination Performance of Previous Graphene-Based Membranes

Filtration mode	Selective layer type	Materials	Water flux ($L\ m^{-2}\ h^{-1}$)[a]	Rejection rate (%)[b]	NaCl feed (M)	Fabrication method	Ref
RO	Graphene	Shear aligned GO	35[c]	33	0.034	Doctor blade	67
		GO/graphene	29[c]	53	0.017	Pressure filtration	92
		GO/graphene	34[c]	72	0.017	Pressure filtration	92
		GO/graphene	36[c]	88.3	0.017	Pressure filtration	92
		rNPGO	239.6[c]	40	0.02	Vacuum filtration	23
		rGO	9.2[c]	69	0.02	Vacuum filtration	23
		CCG	2.5	92	0.008	Vacuum filtration	93
		Pressurized GO	68	55	0.008	Vacuum filtration	81
		Pressurized GO	56	86	0.008	Vacuum filtration	81
		Pressurized GO	43	97	0.008	Vacuum filtration	81
		HLGO	19[c]	10	1	Vacuum filtration	94
		GO	32.8	71	0.01	Vacuum filtration	82
		GO	28.8	52	0.1	Vacuum filtration	82
		GO	19.9	33	0.5	Vacuum filtration	82
		K-rGO	3.6	91	0.017	Vacuum filtration	95
	Graphene-composite	GO-porphyrin	7	25	0.034	Vacuum filtration	96
		GO-TBO	20.2	81	0.01	Vacuum filtration	82
		GO-TBO	14.9	70	0.1	Vacuum filtration	82
		GO-TBO	8.4	48	0.5	Vacuum filtration	82
		rGO−CNT	84	42	0.005	Vacuum filtration	97
		PVA-GO100FLG	17.3	85	0.034	Spray coating	98
		PVA-GO35FLG	21.9	83	0.034	Spray coating	98
		GNM/SWNT	488	86.3	0.034	CVD	99
FO	Graphene	PCGO	0.5	97	0.1	Vacuum filtration	100
		GLG	2.25	75	0.001	Vacuum filtration	101
		GLG	2.26	82	0.01	Vacuum filtration	101
		GLG	2.23	78	0.1	Vacuum filtration	101
		FGOM	0.56	99	0.1	Filtration and plasma treatment	102
	Graphene-composite	KCl-GO	0.1	95	0.25	Drop casting	80
		GNM/SWNT	550	98.1	0.5	CVD	99
		UiO-66−2/GO-1	29.16	85	2	Vacuum filtration	103

[a]Water flux in the presence of salt. [b]Rejection rates for NaCl. [c]Pure water flux.

GO-based membranes can offer several distinct advantages as RO membranes. First, the layered GO membranes allow rapid water transport through nonoxidized domains, nearly frictionless, while the narrow interlayer spacing rejects small salts by size exclusion, therefore, interlayer structure control has intensively been researched.[34,50,80] Li et al. introduced the precise control of interlayer spacing by external pressure regulation (Figure 3B).[81] Typical GO consists of abundant oxygen-containing groups, leading to the swell of the interlayer channels (up to ∼2 nm of *d*-spacing) in aqueous conditions.[35] Thus, the interlayer structure of the GO membrane was regulated by external pressure, resulting in the narrowed interlayer channel (below 0.65 nm). The regulated GO membrane exhibited enhanced NaCl rejection of 97% with water permeance of 25 $L\ m^{-2}\ h^{-1}\ bar^{-1}$ compared to low rejection of bare GO (<20%). Additionally, the interlayer nanochannel structure (dimension or functionality) of GO can be easily tuned through nanointercalators.[50,82] Guan et al. demonstrated GO membrane intercalated functional molecules for tuning of the interlayer structure as shown in Figure 3C.[83] The various porphyrin-based macrocyclic molecules with different functional chains include phenyl, hydroxyl, carboxyl, sulfonic acid, or fluorine groups in the GO laminates. The porphyrin molecules interact with GO nanosheets through pi-pi interaction, narrowing the free spacing in the interlayer channels, moreover, the functional groups of intercalators created high energy barriers for ion (Na^+) transport. As a result, the membrane showed an increased salt rejection of 95% with a slightly decreased water permeance of 0.9 $L\ m^{-2}\ h^{-1}\ bar^{-1}$.

Second, chlorination of feedwater is the most convenient method to prevent biofouling, therefore, chlorine resistance is critical for desalination membranes.[77,84] However, the PA structure is prone to degradation by chlorine attacking amino groups of PA, in contrast, GO with oxygen-containing groups is stable under oxidative conditions including the presence of chlorine.[84,85] Lastly, the abundant oxygen-containing groups enable GO to be dispersed in water, which is advantageous for using green solvents, considering the regulation of the usage of toxic organic solvents in manufacturing industries,[18,86,87] while the graphene sheets are required to be cross-linked to avoid the expansion of interlayer spacing by the intercalated solvents.[88,89]

The multilayered graphene membranes have been intensively researched in recent years and showed feasibility as desalination membranes, however, they have still faced some challenges in the fields, specifically, lower rejection of NaCl (<99%) despite higher water permeance (Figure 3D and Table 2).[23,67,80−82,90−103] The properties are attributed to the swell or deformation nature of GO in aqueous conditions under external pressure, resulting in relatively large nanochannels compared to dense polymeric membranes.[104] As observed in the polymer membranes, the graphene membranes also face a

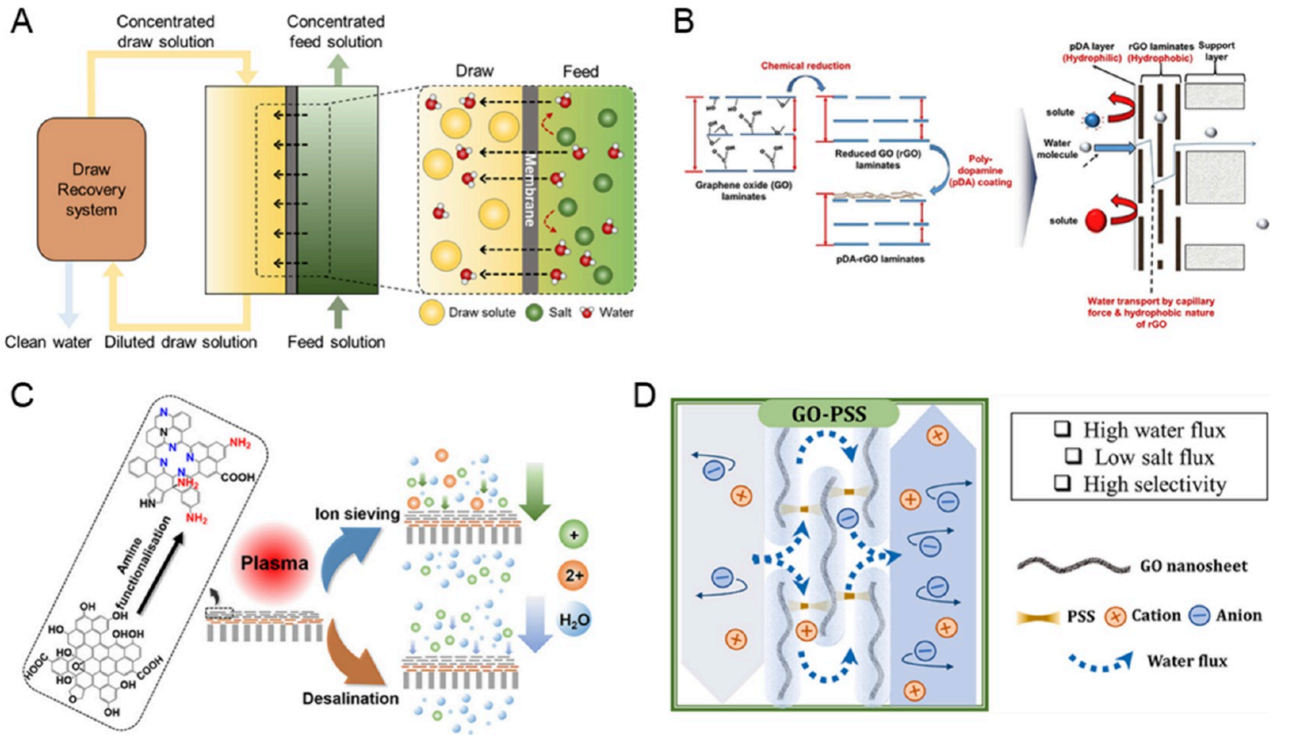

Figure 4. (A) Schematic of the forward osmosis process. (B) Schematic of the reduced graphene oxide membrane coated with polydopamine. Reprinted with permission from ref 111. Copyright 2017 Elsevier. (C) Schematic of functionalized graphene oxide membranes through plasma processing. Reprinted with permission from ref 102. Copyright 2021 American Chemical Society. (D) Schematic of separation mechanism through GO−PSS membrane. Reprinted with permission from ref 115. Copyright 2022 Elsevier.

trade-off between rejection and water permeance because high rejection for salt can be achieved by the narrow interlayer spacing, but the permeance decreases as the channel size decreases. In addition, the thickness of the selective layer of polymer membrane is extremely thin in the range of several tens of nanometers, while the high aspect ratio of graphene forms much longer diffusion pathways through the ultrathin graphene layers.[94] On the other hand, thick graphene membranes (several hundreds of nanometers) have often been demonstrated to increase salt rejections.[82] Unfortunately, the thick graphene layers result in a significant decrease in water flux despite high operation pressure, which could not be exploited for characteristics of graphene membranes, such as frictionless water transport. Therefore, the GO-based membranes are possibly targeted for rejecting organic matter, divalent ions, and heavy metal ions with high chemical stability, including acidic conditions. These aspects are discussed in later sections.

3.2. Forward Osmosis

The forward osmosis (FO) system consists of three parts; draw solution, feed solution, and semipermeable membrane (Figure 4A). The feed solution, which contains impurities such as salts, is situated on one side of the semipermeable membrane, while the draw solution, with a high concentration of solutes, creates an osmotic gradient on the other side. This gradient drives water molecules from the feed solution to the draw solution through the membrane without external pressure. This mechanism highlights the advantage of FO in utilizing osmotic pressure differences, requiring less energy than RO systems to produce clean water, particularly for highly concentrated ionic solutions. Consequently, FO membranes require high water permeability, low solute permeability, and robust mechanical strength, similar to RO membranes. Additionally, addressing internal concentration polarization (ICP) is important for enhancing the long-term stability of the FO membrane. Conventional polymeric FO membranes often suffer from low water flux and significant ICP due to their dense support layer. Furthermore, the FO system needs an additional step to reconcentrating the diluted draw solution using NF, ultrafiltration (UF), and membrane distillation (MD) processes.[105−109] These processes introduce extra operating costs, equipment installment, and energy consumption. Despite these challenges, the FO system is still considered to be a promising technology for treating high-concentration brine solutions or wastewater.

GO membranes exhibit reduced ICP and higher water permeability owing to their narrow interlayer spacing and abundant hydrophilic functional groups (COOH and OH).[110] However, the commercial application of graphene-based FO membranes is still hindered by challenges such as reverse salt flux due to the swelling effect, low long-term stability, and ICP. Yang et al. reported rGO membrane coated with polydopamine (pDA) for desalination (Figure 4B).[111] The GO membrane was chemically reduced using hydriodic acid (HI) vapors to remove the oxygen-containing groups in GO nanosheets. This reduction resulted in a reduced interlayer spacing, which in turn decreased the reverse solute flux of the membrane and improved its stability in water. Additionally, the formation of hydrophobic nanochannels in the rGO membrane increased its water permeability.[112] Moreover, the application of a hydrophilic pDA coating on the rGO surface further improved the membrane's wettability, resulting in enhanced water flux. Consequently, the pDA-rGO membrane achieved a higher water flux (36.6 L m^{-2} h^{-1}) than commercial polymer

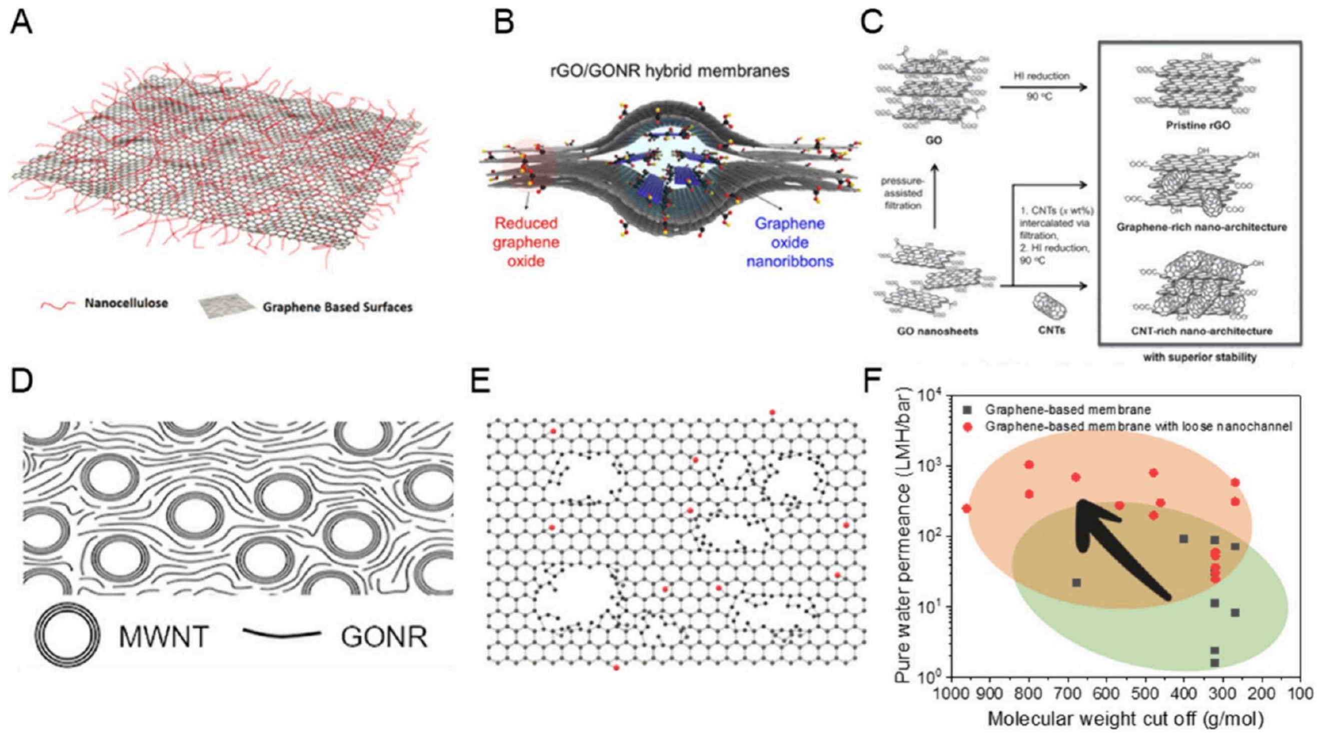

Figure 5. (A) Schematic of GO nanosheets with a cellulose nanofibers for loose nanochannel. Reprinted with permission from ref 137. Copyright 2018 WILEY-VCH Verlag GmbH & Co. KGaA, Weinheim. (B) Schematic of rGO/GONR hybrid membrane. Reprinted with permission from ref 122. Copyright 2019 American Chemical Society. (C) Schematic of the rGO/CNT membrane. Reprinted with permission from ref 127. Copyright 2015 WILEY-VCH Verlag GmbH & Co. KGaA, Weinheim. (D) Schematic of GONR/CNT hybrid membrane. Reprinted with permission from ref 136. Copyright 2022 American Chemical Society. (E) Schematic of a nanoporous graphene membrane. Reprinted with permission from ref 56. Copyright 2021 Elsevier. (F) Comparison of permeance and molecular weight cutoff of graphene-based membrane depending on the presence of additives.

membranes, while demonstrating a relatively low Na^+ ion rejection rate of over 90%. Moreover, the salt rejection of GO-based FO membranes can be enhanced by modifying the surface charge of the GO nanosheets. Qian et al. demonstrated nitrogen-functionalized GO membrane (FGOM) with one-step plasma processing as shown in Figure 4C.[102] Plasma treatment in the H_2/N_2 atmosphere replaced oxygen-containing groups in GO with amine groups (−NH/-NH_2). This modification slightly suppressed the *d*-spacing under wet conditions and imparted a positive charge to the surface, thereby enhancing the rejection of the cations. Consequently, the FGOM exhibited a significantly lower Na^+ ion flux (0.782×10^{-3} mol m^{-2} h^{-1}) compared to the pristine GOM (0.442 mol m^{-2} h^{-1}), resulting in a water/ion selectivity of 2.96×10^3.

Some studies have suggested that using a freestanding GO membrane can reduce ICP to nearly zero, thereby achieving high water flux in the FO system.[113,114] Tong et al. reported a freestanding GO membrane using poly(sodium 4-styrenesulfonate) (PSS) as a polyelectrolyte spacer (Figure 4D).[115] The freestanding GO membrane structure effectively minimized the ICP effect, leading to an enhanced water flux of the GO-PSS membrane. Additionally, the PSS spacer suppressed the swelling of the GO membrane and minimized the reverse salt flux through an exclusion-enrichment effect. The GO-PSS membrane performed better than commercial cellulose triacetate FO membranes, demonstrating a higher water flux (156.5 L m^{-2} h^{-1} with 2 M concentration of draw solution) and lower reverse salt flux (2.3 g m^{-2} h^{-1}). Moreover, the water flux and reverse salt flux of the GO-PSS membrane remained stable for 12 h.

3.3. Nanofiltration

Nanofiltration (NF) is effective for the removal of organic compounds from water and is considered promising in various environmental applications such as wastewater treatment, food processing, and pharmaceutical processes.[116−119] Graphene-based materials have attracted attention for NF membranes due to their molecular separation ability, which arises from the nanosized channels formed by the successive layers of graphene, as well as their low solvent transport resistance due to the frictionless graphene surface. In addition, they exhibit outstanding mechanical and chemical stability, enabling stable membrane separation under harsh conditions, which is crucial for practical applications.[120−122] For these reasons, research into graphene-based membranes for NF has begun. Initially, multilayer GO was explored due to its ability to achieve precise molecular sieving through its narrow interlayer spacing. Qiu et al. first proposed GO membrane as a nanofiltration application.[123] The stacked GO nanosheets on polymeric supports demonstrated effective molecular separation for nanoparticles, including Au, Pt, and dyes. However, GO nanosheets are typically unstable and tend to swell in aqueous conditions due to their abundant oxygen-containing groups.[35,44,124] Therefore, strategies such as reducing GO to rGO or cross-linking GO sheets are employed.[125−128] In particular, the reduction of GO is widely applied to enhance water stability, and various reduction methods including thermal and chemical treatments have been investigated.[126,129,130] The decomposition of oxygen-containing groups can decrease the interlayer spacing of graphene sheets and improve van der Waals interactions between graphene

Table 3. Summary of the Nanofiltration Performance of Graphene-Based Membranes

Type	Material	Water permeance (L m^{-2} h^{-1} bar^{-1})[a]	Rejection rate[b]	MWCO (g/mol)[c]	Fabrication Method	Ref
Graphene-based membrane	Shear-aligned GO	71	MR (90%), MO (95%)	269	Doctor blade	67
	GO/branched PEI	2.4	MnB (>96%), MR (68%)	320	Vacuum filtration	125
	EGO-OSA3	92.9	CR (99.7%)	400	Vacuum filtration	142
	Solvent solvated rGO	88	MnB (99%),	320	Vacuum filtration	143
	Thermal reduced GO	0.3	RhB (96.3%)	479	Vacuum filtration	144
	Base-refluxed rGO	21.8	MB (99.2%), DR81 (99.9%)	676	Vacuum filtration	11
	GO/nylon	11.2	MB (96.3%) MO (99.9%)	320	Electrospray	145
	CGO	1.6	MnB (100%) BB (100%)	320	Vacuum filtration	44
	rGO	11	MnB (95.2%) RhB (97.3%)	320	Pressure-assisted filtration	127
	GONR	8	MR (99.9%)	269	Bar-coating	146
	dGO	30	MnB (99.4%)	320	Slot-die	26
Graphene-based membrane with loose nanochannel	Mesoporous GO	250	EB (90%)	961	Vacuum filtration	147
	Turbostratic nanoporous graphene	400	MB (91.4%)	800	Vacuum filtration	131
	TMC-cross-linked GO	276	MnB (66%), R-WT (95%)	567	LbL deposition	148
	KOH-activated nanoporous GO	36.5	MnB (94%) BB (>93%)	320	Vacuum filtration	21
	UIO-66/rGO	30.6	RhB (95%), MnB (98.7%)	320	Pressurized filtration	133
	ZnO/rGO	300	MB (98.2%)	461	Vacuum filtration	149
	rGO/MWNT	52.7	MnB (99.8%), RhB (100%)	320	Pressure-assisted filtration	127
	GO/CNF	200	RhB (100%)	479	Vacuum filtration	137
	Nanostrand/GO	695	RhB (87%)	679	Vacuum filtration	112
	GONR/rGO	312.8	MR (>99%), MO (95%)	269	Vacuum filtration	122
	SWCNT/GO	800[d]	RhB (97.4%)	479	Vacuum filtration	150
	MXene/GO	25	MnB (99.5%) BB (100%)	320	Vacuum filtration	12
	SFGO	1048	MB (99%)	800	Vacuum filtration	151
	FNG	586	MR (94.2%) MnB (99.1%)	269	Vacuum filtration	18
	MWNT/GONR	60	MnB (97.6%)	320	Slot-die	136

[a]Pure water permeance. [b]Representative probe molecules used for filtration test. [c]Molecular weight cutoff: Molecular weight at 90% rejection. [d]Water permeance in the presence of solute.

layers, preventing swelling in aqueous solution.[131,132] However, this treatment could excessively reduce the interlayer spacing and block the nanochannels, leading to a significant decrease in water permeance.

Therefore, research has increasingly focused on forming loose nanochannels to enhance permeance.[88,97,112,122,127,133−136] Xiong et al. constructed GO nanosheets with a network of cellulose nanofibers (CNFs) (Figure 5A).[137] To assemble GO and CNF, the GO/CNF mixture was placed in an oven for 12 h at 90 °C. GO/CNF thin films were fabricated by vacuum filtration with polymer substrates. The GO/CNF membranes with various thicknesses showed fast water permeance of 200−1000 L m^{-2} h^{-1} bar^{-1} with separation performance for RhB and 5 nm gold nanoparticles. Huang et al. also achieved the formation of loose nanochannels by intercalating nanostrands between rGO layers.[112] They prepared the GO/nanostrands membrane by mixing GO and positively charged copper hydroxide nanostrands (CHNs) in solution, followed by vacuum filtration. The membrane was then reduced using hydrazine as a chemical-reducing agent, and CHNs were dissolved to create a nanostrand-channeled rGO membrane. These nanostrands created a narrow nanochannel network structure between the rGO sheets, leading to a 10-fold enhancement in permeance without sacrificing rejection. However, the use of nanostrands to form loose nanochannels can disrupt the alignment of the graphene sheets. Consequently, research has expanded to include homogeneous carbon-based composites to create loose nanochannels without this drawback.

Cho et al. developed a hybrid membrane of rGO and graphene oxide nanoribbon (GONR) that forms nanochannels without disturbing the stacking of rGO (Figure 5B).[122] While nanochannels were formed by intercalating GONR, the oxygen-containing groups attached to the GONR surface enhanced the electrostatic interactions with filtered molecules. As a result, the hybridization of rGO and GONR produced a synergistic effect, improving both the water flux and dye rejection. Similarly, Goh et al. prepared rGO/CNT composite membranes by hybridizing GO with multiwalled CNT (MWNT) and then reducing the GO/MWNT hybrid material

https://doi.org/10.1021/acsenvironau.4c00088
ACS Environ. Au 2025, 5, 35−60

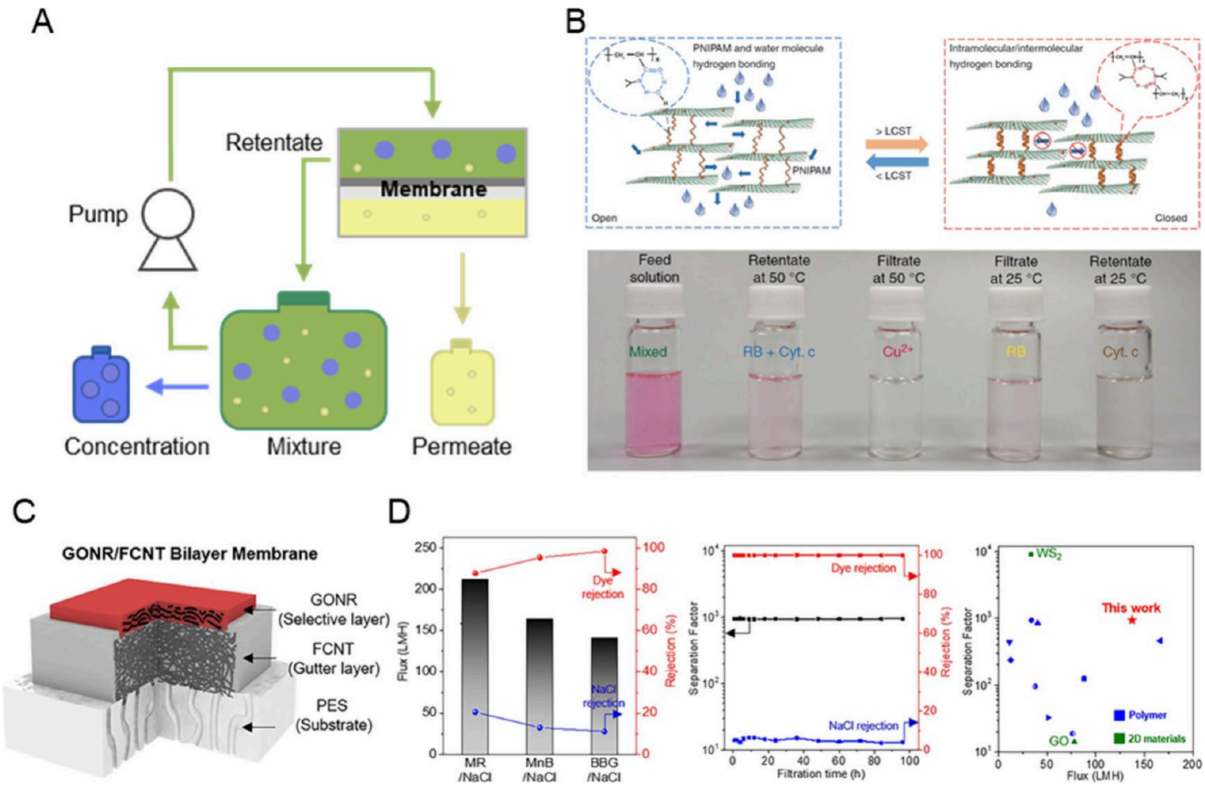

Figure 6. (A) Schematic of the diafiltration process. (B) Schematic of temperature-responsive graphene membrane and the photographs of the mixed feed solution and permeate solution at different temperatures. Reprinted with permission under a creative commons CC BY 4.0 from ref 160. Copyright 2017 Springer Nature. (C, D) Schematic of GONR/FCNT bilayer membrane and dye/salt diafiltration performance. Reprinted with permission from ref 22. Copyright 2021 Elsevier.

(Figure 5C).[127] The intercalation of MWNT prevented the restacking of GO sheets during the reduction process, allowing the formation of nanochannels. This approach enhanced water permeance and stability, maintaining rejection rates.

In addition to 2D GO-based materials, loose nanochannels can also be formed within 1D carbon materials. Kim et al. fabricated a membrane by hybridizing GNRs with CNTs (Figure 5D).[136] By controlling the oxidation time of CNTs, they partially unzipped them into GNRs, creating a GNR/CNT hybrid structure. The intercalation of CNTs formed nanochannels, resulting in a rapid water flux. Alternatively, there are methods to create additional nanochannels by forming pores without intercalation within the interlayer.[56,138−141] Kang et al. prepared nanoporous rGO membranes through pore activation using thermal annealing (Figure 5E).[18,56] The formed nanopores significantly increased water permeance by reducing the transport pathway for water while also sieving molecules larger than the pores or interlayer spacing. As a result, they achieved ultrafast water permeance of 586 L m^{-2} h^{-1} bar^{-1} and a low MWCO of 269 Da.

Figure 5F and Table 3 compare the performance of conventional graphene-based membranes with those incorporating loose nanochannels (refs 11, 12, 18, 21, 26, 44, 67, 112, 122, 125, 127, 131, 133, 136, 137, 142−151). These approaches, including the formation of loose nanochannels or pores, have proven to effectively enhance water permeance while maintaining separation ability. In most cases, one-dimensional (1D) materials are intercalated to increase the solvent permeance. While other 2D materials such as MXene or MoS_2 are incorporated in hybrid forms to improve selectivity, the increase in permeance is not as significant compared to the addition of 1D materials, or the permeance can even decrease because 2D materials typically act as barriers for small molecules.[12,152]

3.4. Diafiltration

Diafiltration is a separation process in mixture systems that uses membranes to separate different solutes or concentrate specific components. It plays a crucial role in various industries, including pharmaceuticals and biotechnology, food and beverage, chemicals, textile, and environmental industries, and is primarily used to purify products such as dyes, protein, antibiotics, vaccines, and enzymes.[136,153−155] It is employed to remove small impurities (such as salts, sugars, heavy metal ions, organic pollutants, and electrolytes), which not only enhances the purity of the product but also enables resource recovery and safe disposal of pollutants, thus playing a significant role in environmental protection.[156] Specifically, high concentrations of mixed solutions combining salts and dyes are used to achieve effective coloring. Consequently, separating and reusing ions and dyes from the mixed solution after the process are crucial for environmental conservation.

In the diafiltration process, the purpose is to allow smaller solutes to permeate quickly while filtering out larger solutes (Figure 6A). Graphene-based membranes are considered promising for diafiltration due to their molecule-sieving advantages, leading to several studies in this field. In particular, the properties of GO membranes, such as roughness, interlayer spacing, lateral size, and wettability, can be tuned by adjusting external factors such as pH, solvent, ion concentration, electrical field, temperature, functionality, and drying.[48,157−161] Various research studies have been conducted to improve

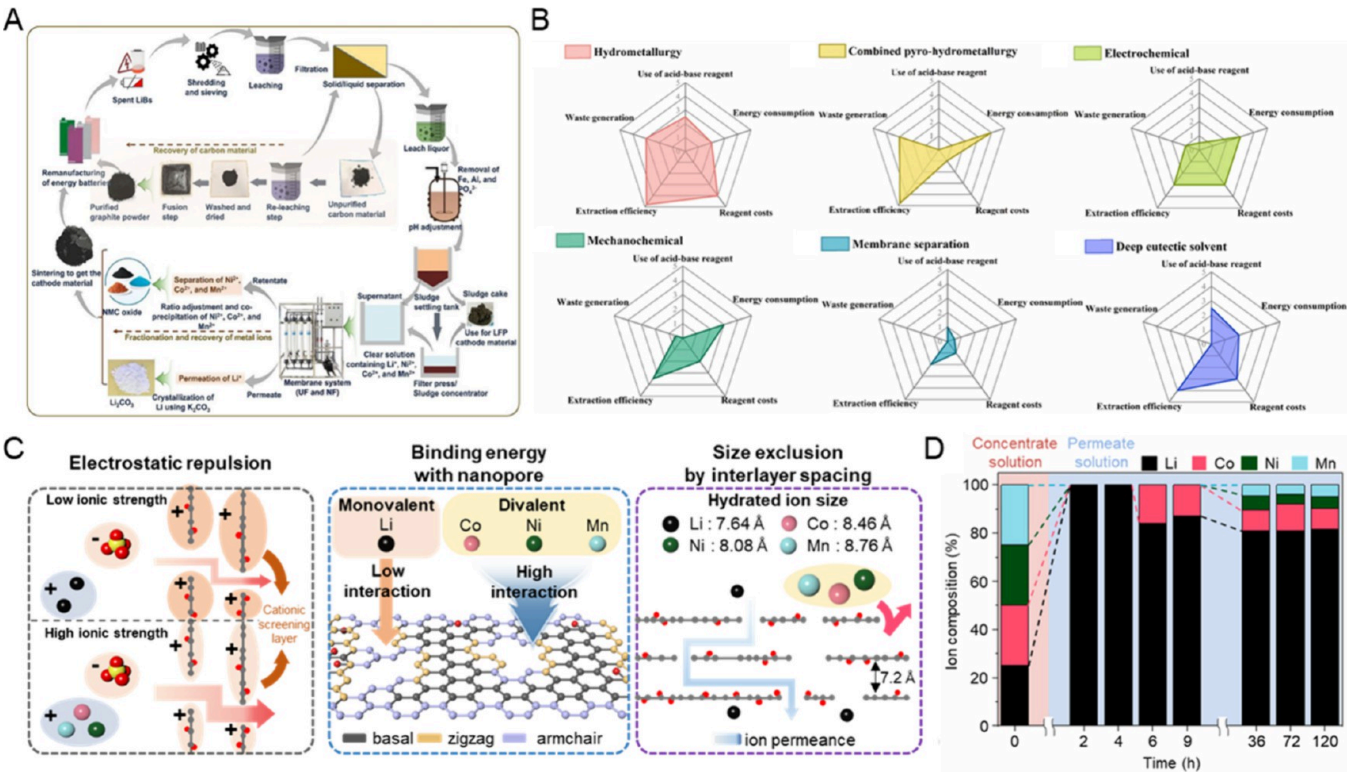

Figure 7. Rare metal recovery from spent ion batteries. (A) Schematic of membrane-integrated hybrid technology for recycling materials from spent Li batteries. Reprinted with permission from ref 167. Copyright 2023 Elsevier. (B) Radar charts ranking various parameters for lithium recovery methods from spent batteries. Reprinted with permission from ref 170. Copyright 2024 Elsevier. (C) Various factors related to metal ion recovery performance of graphene-based membranes. (D) Forward osmosis ion separation test results (molar composition of the ions) for the nanoporous multilayer graphene oxide membrane. Reprinted with permission from ref 25. Copyright 2023 Elsevier.

separation performance by utilizing these tunable properties. Liu et al. prepared a GO-based membrane by cross-linking poly(*N*-isopropylacrylamide) chains between GO sheets (Figure 6B).[160] They mixed GO with the monomer in solution and polymerized it to form a membrane via pressure-driven filtration. Due to the tunable lamellar spacing responsive to temperature changes, the membrane exhibited increased water permeability and demonstrated the ability to separate three substances (Cu^{2+}, RB, Cyt.c) using a single GO-based membrane. Since diafiltration processes are closely related to industrial separation, it is also important to develop membranes suitable for practical applications. Some research for the fabrication of membranes with properties for industrial approaches including scalability, mechanical strength, and long-term stability has been reported. Choi et al. developed a membrane using GONR as a selective layer and Functionalized CNT (FCNT) as the gutter layer (Figure 6C, D).[22] The GONR/FCNT membrane exhibited precise separation performance due to the well-stacked GONR, while the FCNT gutter layer enhanced mechanical strength, ensuring membrane stability under high-pressure operation and long-term operation. In a cross-flow system, the diafiltration performance for BBG dye and NaCl was tested at a high pressure of 8 bar, showing a high water flux of 138 L m^{-2} h^{-1} and a high separation factor of 950.

3.5. Metal Recovery and Extraction (Noble Metal or Rare Metal)

As interest in electric vehicles continues to grow, the use of lithium-ion batteries (LIBs) has increased, resulting in a significant increase in the number of spent batteries. By 2030, it is estimated that 110,000 tons of spent batteries will be generated.[162] This could contribute to resource depletion and environmental pollution; therefore, recovering rare metal ions from batteries is becoming increasingly important. Currently, two methods are commonly used to recover metal ions from spent batteries: pyrometallurgy and hydrometallurgy.[163−167] The pyrometallurgy process involves the high-temperature treatment of batteries to extract metal ions, which is advantageous for large-scale operations. On the other hand, the hydrometallurgy process dissolves pretreated spent batteries in chemical solvents to extract metal ions, offering higher recovery efficiency. However, both methods require substantial energy and costs to separate metal ions from spent batteries.[167−169]

To address these challenges, the integration of membrane technology into the process of recovering metal ions from spent batteries can reduce the energy and cost requirements. Kumar et al. proposed a pressure-driven membrane-based hybrid system that combines the hydrometallurgical process with membrane technology to recover metal ions from spent batteries in an environmentally friendly and efficient manner (Figure 7A).[167] In traditional hydrometallurgical processes, separating valuable metal ions (Li^+, Co^{2+}, Ni^{2+}, and Mn^{2+}) from impurities, such as Fe, Al, and phosphates, is difficult. These multimetal solutions require large amounts of reagents and energy for separation, making it challenging to recover Li^+ alongside Co^{2+}, Ni^{2+}, and Mn^{2+} using conventional processes. However, the membrane-based hybrid system can separate impurities, such as $Fe(OH)_3$, $Al(OH)_3$, and iron phosphate using a UF membrane. The valuable metal ions (Li^+, Co^{2+},

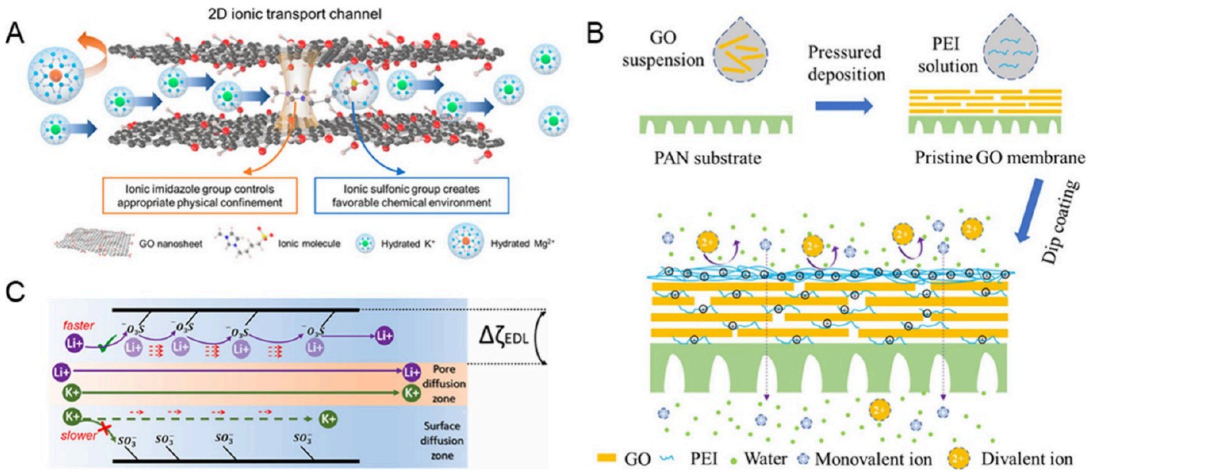

Figure 8. Metal ion extraction from brine and seawater. (A) Schematic of ionic molecule inserted GO membrane for separating Li^+/divalent ions. Reprinted with permission from ref 186. Copyright 2021 American Chemical Society. (B) Schematic of the GO-PEI membrane for separating Li^+/divalent ions. Reprinted with permission from ref 187. Copyright 2022 Elsevier. (C) Schematic of PSS-incorporated GO membrane for Li^+/monovalent separation. Reprinted with permission from ref 188. Copyright 2023 Elsevier.

Ni^{2+}, and Mn^{2+}) in the supernatant can then be separated using a pressure-driven NF membrane, which separates Li^+ in the permeate stream while retaining divalent metal ions (Co^{2+}, Ni^{2+}, and Mn^{2+}). This hybrid approach demonstrates improved efficiency over traditional processes.

Figure 7B presents a comparative summary of various recovery methods in lithium recovery processes, highlighting their acid−base reagent use, energy consumption, reagent costs, extraction efficiency, and waste generation in radar charts.[170] The membrane method shows advantages in terms of lower energy consumption, reduced environmental impact, and high selectivity for Li^+ compared with other recovery processes. Furthermore, graphene-based membranes are highly stable under acidic or alkaline leaching conditions compared to typical polymeric membranes, which are advantages for the recovery of metal ions.[165,171−173] However, membrane-based research on ion recovery from batteries is still in its early stages.

Kim et al. reported using a nanoporous multilayer graphene oxide (NMG) membrane fabricated through the hot-press method to recover ions from spent lithium batteries. The hot-press method was utilized to control the interlayer spacing and pore size/density of the graphene membrane. The NMG membrane exhibited different ion permeation phenomena depending on ion concentration (Figure 7C).[25] In low-concentration solutions, the NMG membrane showed multivalent ion selectivity due to electrostatic repulsion of the electrical double layer. Conversely, in mixed or high-ionic solutions, the NMG membrane demonstrated high lithium selectivity due to size exclusion and the binding energy between graphene and metal ions. The NMG membrane was also applied to a continuous FO system (Figure 7D). High lithium selectivity was initially maintained until 6 h. However, over time, the lithium selectivity was decreased due to the swelling effect of the NMG membrane. These findings show the potential of GO membranes for the continuous recovery of rare metal ions from spent batteries. However, further studies are still needed to maintain fast ion permeability and high ion selectivity for the commercial use of GO membranes for ion recovery from spent batteries. Particularly, rigid interlayer spacing is critical for the separation of monovalent and multivalent ions from mixture solutions, such as K^+ or Li^+ from Mg^{2+} in brine, Li^+ recovery from metal-ion-rich wastewater, and the recycling of metal ions from acidic radioactive waste.[174−177] Of course, recovering metal ions from spent batteries is just one of the applications using graphene membranes. The recovery of valuable metal ions through the membrane process is becoming increasingly important due to other electrochemical applications such as fuel cells and electrolysis, in which precious metals including Pt, Ir, Ru, Ni, Co, etc. are used.[178,179] Therefore, future research is needed to enhance the chemical stability of graphene membranes and optimize their selectivity for specific ions for various industrial applications.

As the demand for lithium ions rapidly increases, extensive research is being conducted on various methods for securing lithium supplies. While the recovery of lithium ions from spent batteries is still in its early stage of development, methods for extracting lithium ions from brine and ore have been studied for a long time. Especially, seawater contains approximately 230 billion tons of lithium, making it a promising and significant source of this valuable metal.[180,181] The lime-soda evaporation process is a conventional method for extracting lithium ions from brine using solar evaporation.[182,183] However, the concentrated brine is limited and time-consuming to evaporate. Therefore, various techniques for concentrating and extracting lithium ions from lower-concentration seawater and wastewater have been developed. The lithium concentration in seawater is low in the range from 0.17 to several hundred ppm, coupled with various other ions such as sodium and magnesium.[184,185] Therefore, extracting lithium ions from seawater necessitates highly selective lithium separation technologies. To address this challenge, membrane-based lithium extraction processes have become significantly prominent due to their energy efficiency and superior lithium selectivity.

Polymeric membranes have generally been used in commercial applications, but controlling the precise pore size for Li^+/other divalent ion selectivity remains challenging. On the other hand, the well-defined interlayer structure of GO is appropriate for the mono/divalent ion separation, however, GO-based membranes tend to expand the interlayer spacing in

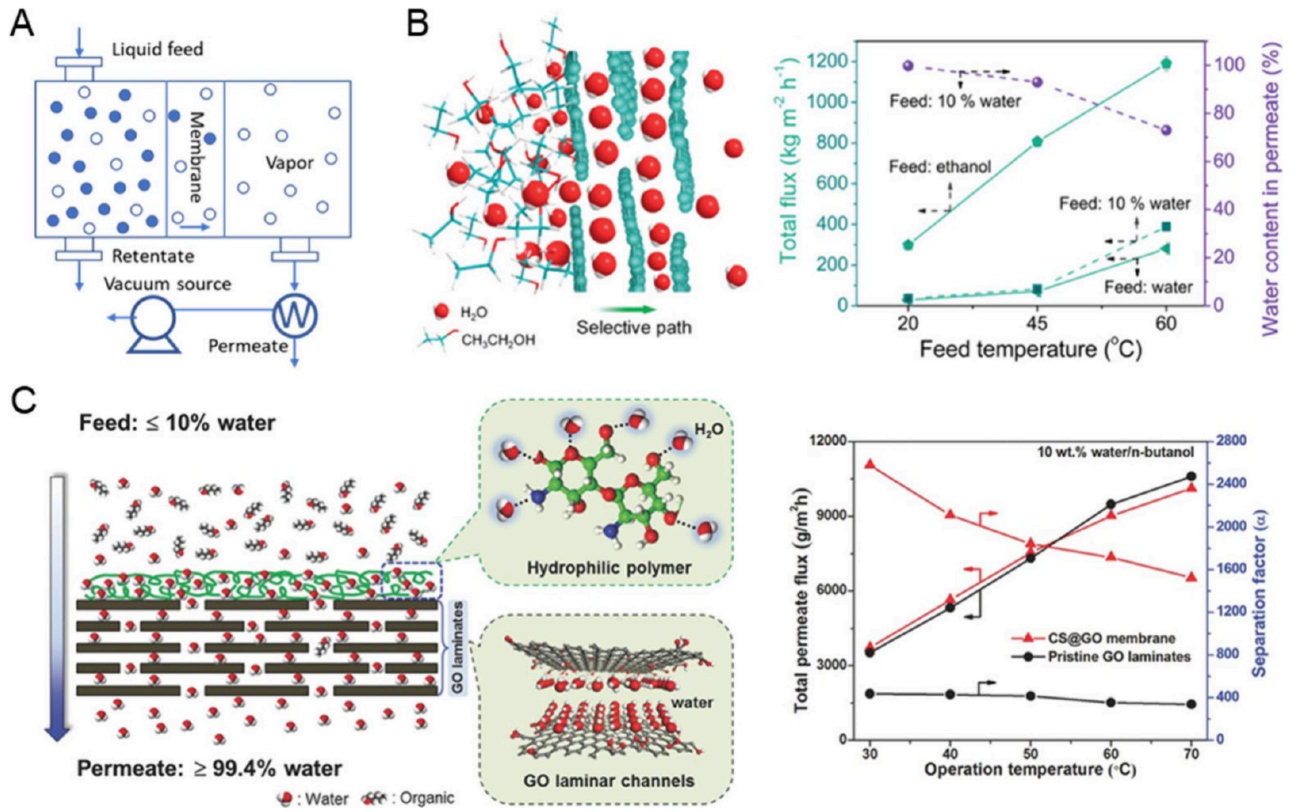

Figure 9. (A) Schematic for the pervaporation mechanism. (B) Schematic for ethanol dehydration of an rGO/CS-derived carbon membrane and its ethanol dehydration performance according to feed temperature. Reprinted with permission from ref 195. Copyright 2020 WILEY-VCH Verlag GmbH & Co. KGaA, Weinheim. (C). Schematic of butanol dehydration process using GO/CS polymer membrane and its performance with 10 wt % water/n-butanol solution. Reprinted with permission from ref 201. Copyright 2015 WILEY-VCH Verlag GmbH & Co. KGaA, Weinheim.

the aqueous solutions due to the abundant oxygen-containing groups. Therefore, it is imperative to develop GO-based membranes that maintain stable interlayer spacing in aqueous conditions, while enabling precise control over the interlayer distance to achieve high ion selectivity.

Zhang et al. reported ionic GO (i-GO) membranes by incorporating ionic molecules to create biomimetic 2D ionic transport channels (Figure 8A).[186] Imidazole groups regulate the physical constraints of the ion transport channels to ensure the size exclusion of divalent ions. The i-GO membrane exhibited a much smaller expansion in *d*-spacing (from 8.5 to 9.3 Å), owing to the stabilizing interactions from the imidazole group. Additionally, the ionic imidazole groups hindered the permeation of divalent ions due to the steric hindrance exclusion effect. Consequently, the i-GO membrane showed a much higher lithium ion permeation (~1.29 mol m^{-2} h^{-1}) than magnesium ion permeation (~0.15 mol m^{-2} h^{-1}), resulting in a Li^+/Mg^{2+} selectivity of 8.6. To further enhance lithium selectivity, Zhang et al. demonstrated GO-PEI membrane with controlling surface charge and interlayer spacing of GO membrane using PEI (Figure 8B).[187] GO-PEI membrane was fabricated by employing PEI in a layer-by-layer assembly. The *d*-spacing of the GO-PEI membrane increased by ~1.0 Å compared to pristine GO, the cross-linking between GO layers effectively suppressed the swelling effect in aqueous environments. Moreover, the coating of PEI imparted a positive charge to the membrane surface and enhanced its hydrophilicity. The increased interlayer spacing and positive surface charge facilitated the transport of monovalent ions, while hindering the permeation of divalent ions. As a result, the GO-PEI membrane exhibited a significantly improved Li^+/Mg^{2+} selectivity of 37.6, approximately 25 times higher than that of the pristine GO membrane.

Recently, research has also focused on enhancing the selectivity for monovalent ions beyond lithium and divalent ions. Liu et al. reported the freestanding GO-polystyrenesulfonate (PSS) composite membrane (GOM-S) to enhance Li^+/monovalent ions selectivity (Figure 8C).[188] PSS not only acts as a spacing agent to suppress the swelling of the GO membrane's interlayer spacing but also enhances the surface charge density of the GO membrane. Furthermore, the DFT calculation showed that the binding energy of lithium with PSS is lower than those of potassium and sodium, which resulted in increased Li ion permeability in GOM-S. Consequently, the Li^+/K^+ and Li^+/Na^+ selectivities of GOM-S increased to 1.80 and 1.97, respectively. This demonstrates the potential to manufacture membranes with high lithium selectivity among monovalent ions using GO membrane.

3.6. Pervaporation

While the aforementioned applications are mostly used for water treatment, membrane-based technologies such as pervaporation (PV) and membrane distillation (MD) can be applied under specific operating conditions. In PV, mass transfer is driven by the difference in chemical potential between the feed and permeate sides, caused by vacuum pressure or airflow (Figure 9A).[189] PV differs from MD in that PV typically uses hydrophilic membranes to selectively permeate and separate components in a liquid mixture, while MD relies on a temperature gradient to induce vapor

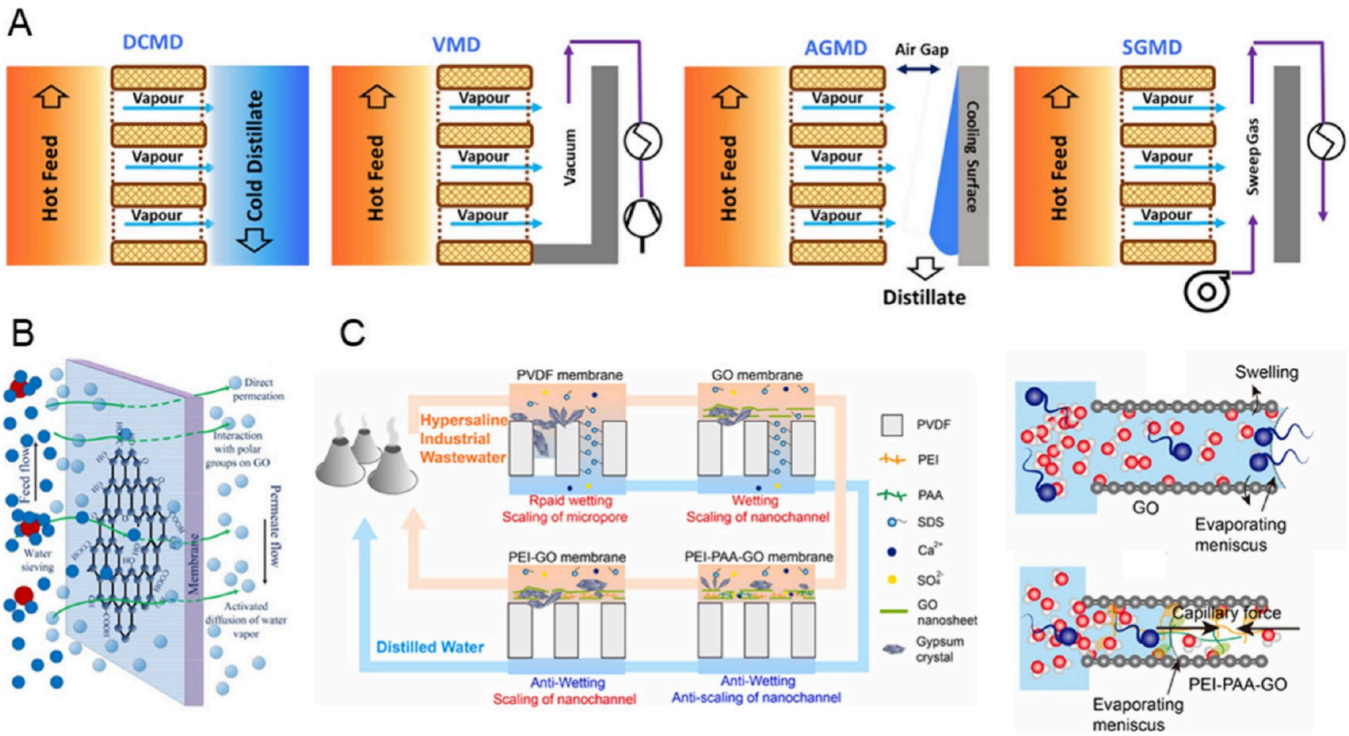

Figure 10. (A) Membrane distillation operation setup; direct contact membrane distillation (DCMD), vacuum membrane distillation (VMD), air gap membrane distillation (AGMD), and sweep gas membrane distillation (SGMD). Reproduced with permission from ref 208. Copyright 2024 Elsevier. (B) Schematic of water vapor transport in the presence of GO. Reprinted with permission from ref 211. Copyright 2015 Elsevier. (C) Schematic of wetting and scaling properties using PVDF, GO, PEI-GO, and PEI−PAA-GO membranes and mechanism of wetting difference for GO and PEI−PAA-GO membranes. Reprinted with permission from ref 215. Copyright 2024 Elsevier.

permeation through a hydrophobic membrane.[190] The permeating molecules are desorbed from the membrane, taking a phase transition to vapor. Especially, the pervaporation system has the advantages of organic contaminant removal, and azeotrope breaking.[191−193]

GO is promising for a water-selective PV membrane due to its ultrathin 2D structure and multifunctional surface chemistry. In addition, the thickness of graphene-based membranes can be easily controlled by adjusting the coating conditions, and the thickness of the selective graphene layer can affect the PV performance. As the selective layer of graphene is thick, the diffusion pathway is elongated, in addition, the intrinsic defects are possibly covered, which all leads to more increased diffusion resistance for larger solvent molecules, in other words, more water-selectivity.[38,194] Adjusting the interlayer spacing of graphene-based membranes can enhance the selectivity for specific molecules or increase the permeance. Chen et al. reported robust angstrom-channel graphene membranes (ACGMs) by thermal treatment on GO membrane intercalated carbonized chitosan (CS) (Figure 9B).[195] Owing to the angstrom size effect of graphene channels in ACGMs, the membrane demonstrated exceptional ethanol dehydration under PV systems, achieving water flux of 63.8 kg m^{-2} h^{-1} at 20 °C and 389.1 kg m^{-2} h^{-1} at 60 °C for the water containing 90 wt % of ethanol, concentrating ethanol up to 99.9 wt %.

Approaches such as forming polymer composites or functionalizing GO are extensively studied to control interlayer spacing.[196,197] However, the interlayer spacing of GO can be swollen during the membrane operation, therefore, it is necessary to explore methods such as using cross-linking agents and intercalating nanoparticles to mitigate this swelling effect for performance stability during long-term operation.[198,199] Zhang et al. fabricated double-cross-linked GO membranes using CS and trimesoyl chloride (TMC).[198] The membrane showed stable isopropanol (IPA) dehydration performance for up to 100 h with a water flux of 4391 g m^{-2} h^{-1} at 60 °C for a feed containing 90 wt % of IPA, which is attributed to the strong double-cross-linking between GO and CS/TMC.

GO membranes with abundant hydrophilic oxygen-containing groups enable rapid water permeation during the PV process. Water molecules are more likely to be adsorbed on the hydrophilic membrane surface compared to organic solvent molecules due to their higher polarity. In addition, smaller water molecules have lower diffusion resistance in GO channels, improving water-preferential permeation.[200] Huang et al. reported that an ultrathin surface water-capturing polymeric layer (<10 nm) coated on GO membrane significantly improves water permeation in butanol dehydration, achieving over 10,000 g m^{-2} h^{-1} of water flux (Figure 9C).[201] Hydrophilic CS polymer, with its strong water sorption ability, effectively facilitates the transport of water molecules. To enhance the water permeation of the GO membranes, methods such as functionalizing the hydrophilic group and incorporating the hydrophilic nanoparticles are being developed.[202,203]

Despite their water-selective properties, various simulation studies predict that alcohol-selective permeation could occur in multilayer graphene due to poor water affinity induced by the low amount of oxygen-containing groups.[204,205] The decomposition of oxygen-containing groups can cause the interlayer spacing to close, which suppresses solvent permeation; thereby, the alcohol selectivity has hardly been realized in

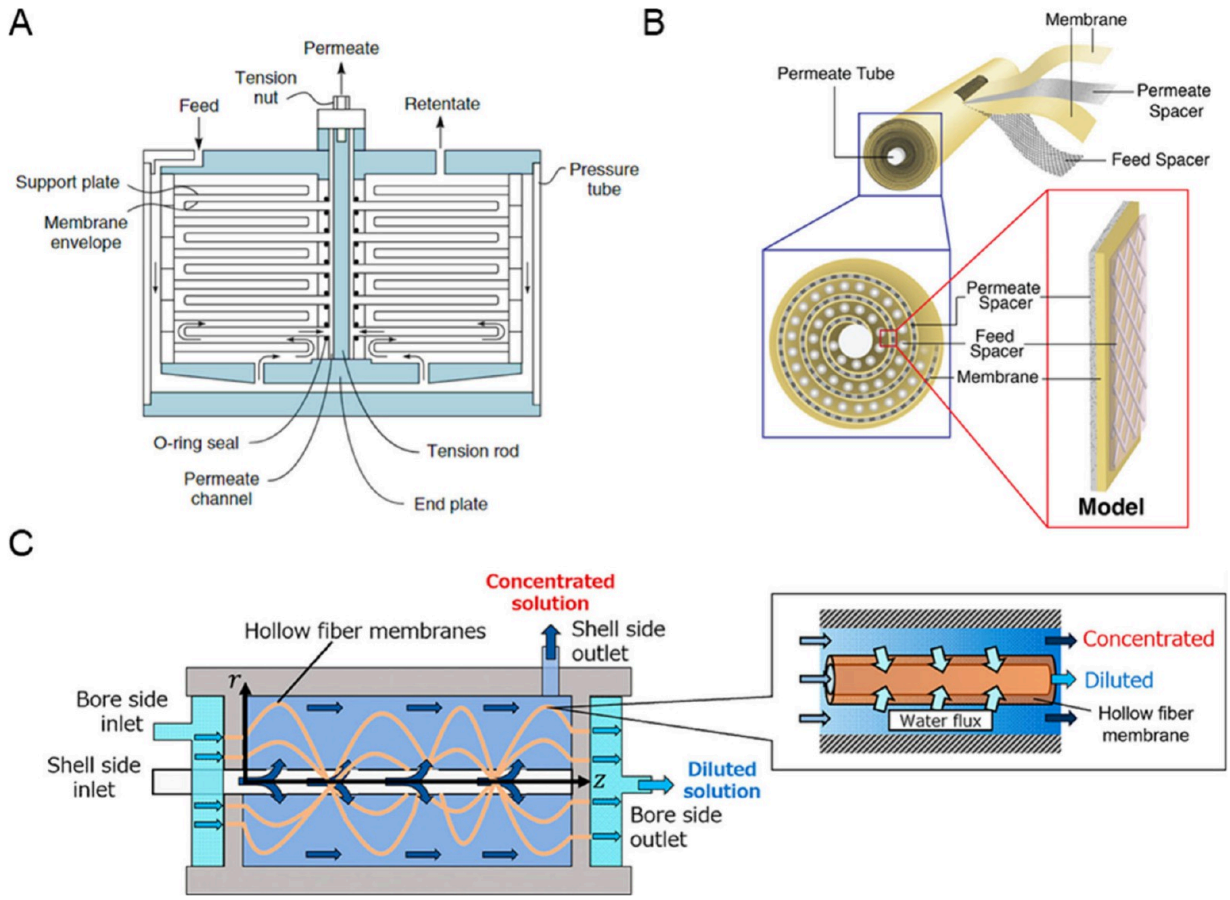

Figure 11. Schematic illustrations of the membrane module type. (A) Plate-and-frame module. Reproduced with permission from ref 217. Copyright 2012 John Wiley & Sons. (B) Spiral-wound module. Reprinted with permission from ref 218. Copyright 2021 Elsevier. (C) Hollow fiber module. Reprinted with permission from ref 220. Copyright 2019 American Chemical Society.

the experimental conditions. However, this approach could be effective for water concentration (or alcohol extraction) from aqueous organic solvents with a high water content. While separation performance in mixed substances has not yet been reported, previous studies have shown that in crystalline porous graphene membranes, water permeation is significantly reduced compared to other organic solvents, implying the potential of alcohol-selective graphene membranes.[37,131]

3.7. Membrane Distillation

Membrane distillation (MD) is a separation process driven by heat, where a hydrophobic membrane blocks the liquid phase while allowing the vapor phase to pass through.[206] MD is a promising separation technology for desalination and wastewater treatment due to its minimal energy consumption and cost efficiency, achieved through mild operating conditions.[207] Among the four main MD configurations in Figure 10A, direct contact membrane distillation (DCMD), which is feed and permeate direct contact on both sides, is commonly used due to its ease of setup and low energy consumption.[208,209] In vacuum membrane distillation (VMD), applying a vacuum on the permeate side increases the driving force for distillation and leads to a higher flux. Air gap membrane distillation (AGMD) involves an air gap between the membrane and the condensation surface, which reduces heat losses and makes the process more energy efficient. Sweeping gas membrane distillation (SGMD) involves a sweep gas that flows along the permeate side of the membrane to enhance mass transfer by carrying away the vapor as it permeates through the membrane.[208,209]

Graphene-based membranes exhibit faster permeance in MD operations compared to conventional polymer membranes.[210] Because the MD membrane is made of macropores and bulk water permeation is hindered by the hydrophobicity of the membrane materials, the addition of a too thick graphene layer can reduce the water permeation. However, the thin graphene layer efficiently serves as a water vapor sorption site while repelling the liquid water molecules (Figure 10B).[211] This structure helps to release water vapors from bulk water by breaking hydrogen bonds, aiding in vaporization. In addition, the high thermal conductivity of graphene-based materials facilitates efficient heat transfer, promoting rapid evaporation.[212]

The graphene layer is an excellent choice for stable MD operation as it acts as a barrier against contamination. Additionally, the graphene layer effectively prevents the wetting phenomenon, ensuring high membrane efficiency even under low surface tension conditions induced by contaminants such as sodium dodecyl sulfate (SDS).[213,214] To further enhance the antiwetting properties, methods such as adjusting interlayer spacing and improving hydrophobicity are also being studied. Lou et al. fabricated the GO membrane by inserting PEI and poly(acrylic acid) (PAA), which retained narrow interlayer spacing and low free volume during the MD operation (Figure 10C).[215] Therefore, the narrow GO channel successfully suppressed the SDS entrance. In the PEI–PAA-

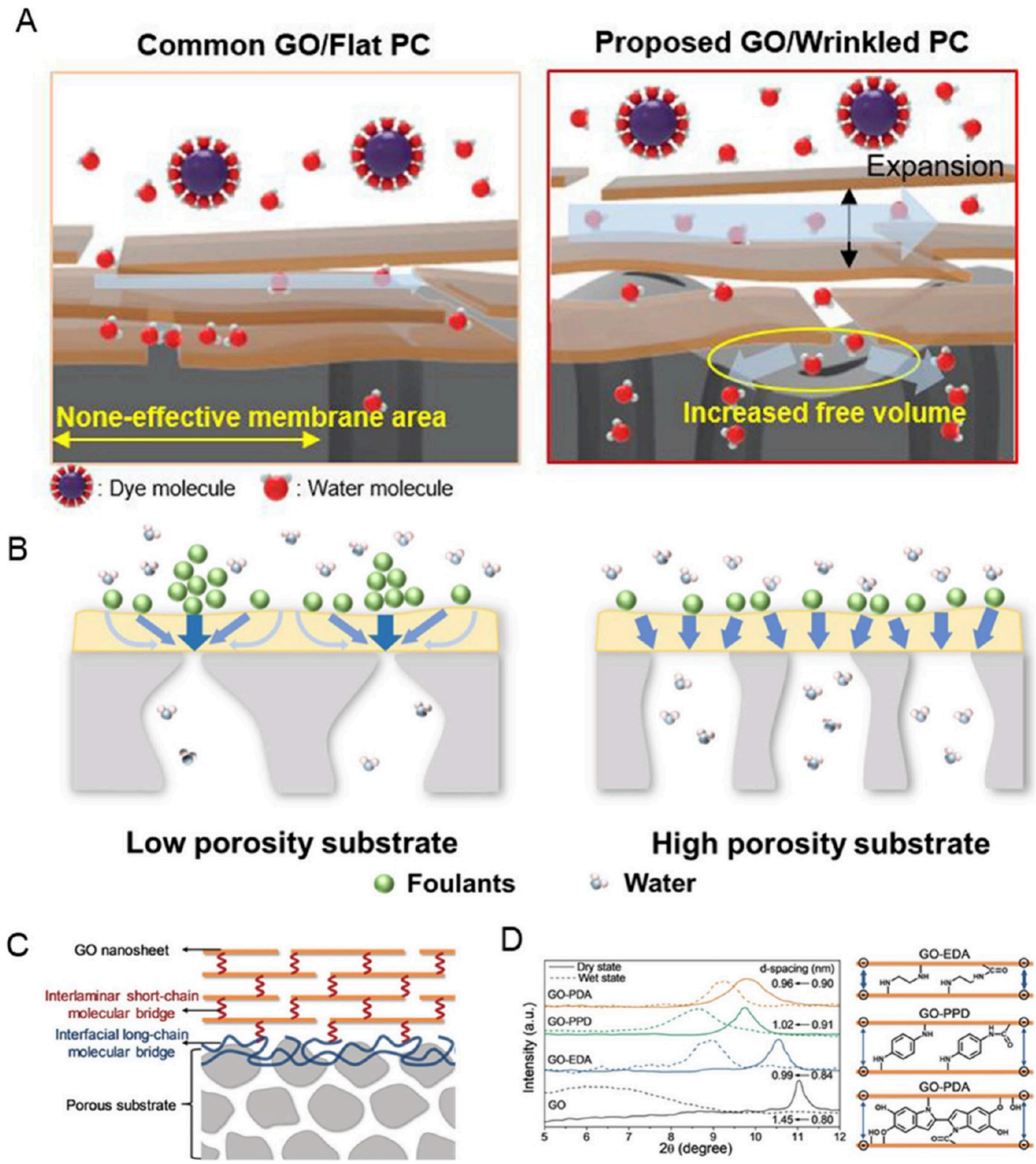

Figure 12. (A) Support structure tuning for the GO membrane fabrication. Reprinted with permission from ref 225. Copyright 2019 Elsevier. (B) Foulant accumulation depending on the porosity of the substrate. Reprinted with permission under a creative commons CC BY 4.0 from ref 227. Copyright 2022 Elsevier. (C, D) Cross-linking approach to enhance adhesion between graphene layers or between graphene and a substrate. Reprinted with permission from ref 228. Copyright 2020 Wiley-VCH Verlag GmbH & Co. KGaA, Weinheim.

modified GO membrane, the interaction between water and the functional groups causes a side-pinning effect, which slows down the desorption and diffusion of water molecules, stabilizing the capillary force. As a result, it becomes harder for SDS to escape, leading to the membrane's antiwetting property. The membrane demonstrated resistance during the MD test with 0.4 mM SDS for 17 h, outperforming the normal GO membrane. In addition, the incorporation of PAA effectively prevented gypsum scaling within the GO nanochannels by chelating the carboxyl groups of PAA molecules with Ca^{2+} ions. Chen et al. reported a plasma-treated nanoporous GO membrane with omniphobic properties by fluoroalkyl grafting.[216] The membrane exhibited a high water flux of 35 kg m^{-2} h^{-1} because of additional water transport channels through the nanopores activated by plasma treatment. Moreover, fluoroalkyl grafting enhanced hydrophobicity, effectively preventing wetting. As a result, the membrane maintained a salt rejection rate of 99.9% in the presence of 0.2−0.4 mM of SDS over 450 h.

4. FUTURE PERSPECTIVES FOR GRAPHENE-BASED MEMBRANES

4.1. Membrane Module Fabrication

Despite the potential of graphene-based membranes, the practical utilization for the industry has not been unresolved because most of the work in their field has been focused on performance enhancement on a laboratory scale. However, industrial separation processes are necessary to expand membrane surface area, hundreds to thousands of square meters, to achieve the desired water treatment on a commercial scale. Therefore, it is crucial to develop systems for packaged membrane modules such as plate-and-frame,

https://doi.org/10.1021/acsenvironau.4c00088
ACS Environ. Au 2025, 5, 35−60

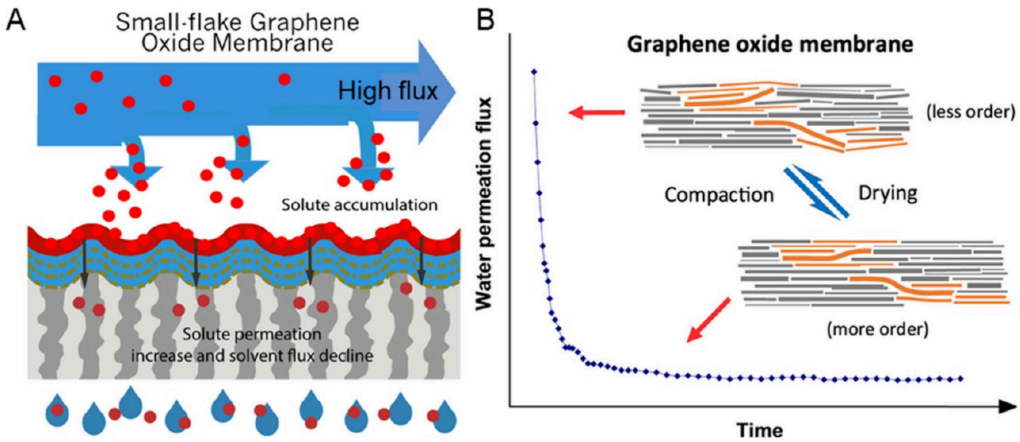

Figure 13. (A) Severe solute accumulation on the GO membrane by ultrafast solvent flux. Reprinted with permission from ref 151. Copyright 2021 Elsevier. (B) Ordering of graphene nanosheets by pressure-assisted compaction. Reprinted with permission from ref 237. Copyright 2017 Elsevier.

spiral-wound, and hollow fiber (Figure 11). The membrane module system can not only increase the effective membrane area but also compact water-treatment facilities, which enable the realization of a commercial membrane process. Plate-and-frame modules are typically composed of alternately stacked membranes and spacers between two end-frames (Figure 11A).[217] The module configuration is favorable for recovering sieved sources during water treatment due to its easy disassembly. However, the packing density (effective membrane area per module) is relatively low compared to other module types, leading to less efficient space utilization.[217] The plate-and-frame module-related graphene membranes have not been reported, even though sheet-type graphene membranes could be easily adapted for the configuration.

The spiral-wound type consists of numerous flat-type membranes, feed spacers, and permeate spacers wound and placed in a tube (Figure 11B).[218] The module has been widely utilized in various applications including RO, UF, and even gas separation operations due to its high packing density and robust design, however, the tightly wound structure leads to the difficulty of cleaning once fouled.[74,219] Recently, GO membranes with this configuration have been rarely attempted and demonstrated, while the module type is commonly used for polymeric membranes.[72]

The hollow fiber module comprises multiple hollow fiber bundles housed in a cylindrical shell (Figure 11C).[220] The type allows for an extremely high packing density, offering a significant effective area within a compact module due to a large number of fine fibers.[217] However, the narrow spacing between the fibers makes them difficult to clean and highly prone to fouling.[221] Scalable GO-based hollow fiber fabrication is relatively challenging compared to other configurations with flat-sheet types. While most existing graphene coating processes are based on shear-induced coating applied to flat substrates, this technique is difficult to implement on hollow fibers. Although some methods have been reported for self-assembling graphene onto amine-treated PVDF fibers, the approaches have not been validated at the module level.[17] To achieve rapid solvent permeation, additional structural controls, such as pore generation, must be applied to graphene. However, the introduction of pores often degrades the graphene coating or stacking quality, making it difficult to achieve uniform coating on small-diameter fibers.[222,223] Moreover, unlike gas separation membranes, fiber-type membranes for solvent treatment require a sufficiently large internal diameter to facilitate the extraction of permeated solvents; however, controlling the diameter of hollow fibers through spinning methods remains challenging.

4.2. Substrate Morphology

GO-based membranes are usually fabricated with a thin-film composite (TFC) structure; therefore, the substrate structure is highly crucial for membrane performance.[224] First, the roughness of support can influence the alignment of the stacked graphene nanosheets (Figure 12A).[225] The interlayer structure of multilayer graphene is the most important element because the interlayer is the main channel for molecular transport. The wrinkled structure of support (high roughness) contributes to increased surface area and better mechanical stability, leading to improved filtration efficiency in terms of solvent permeation.[225] Moreover, the rough surface is beneficial for stable membrane operation with high pressure and cross-flow conditions, which prevent detachment from supports.[22,226] However, the rough surface of the support can enlarge the interlayer spacing of the deposited graphene layer, resulting in a low selectivity for small ions or organic molecules. In particular, an ultrafast membrane accelerates the concentration polarization of filtered molecules, eventually lowering the apparent rejection rates.

Second, the porosity of supports affects fouling behavior as shown in Figure 12B.[227] The more porous structure of the substrate could relieve membrane fouling due to a more uniform flux distribution. The foulants tend to accumulate more in areas in which the flux is higher. Accordingly, porosity control is highly crucial for the antifouling performance, ensuring stable long-term membrane operations. Lastly, strong adhesion between substrates and selective layers is necessary for practical applications because GO-based membranes have faced redispersion or peeling from supports in water. One of the approaches to enhance adhesion is to generate strong covalent bonding by additional treatment on the substrate. Figure 12C, D presents the interface molecular bridge strategy which is capable of robust interfacial connection between the substrate and GO laminates by chemical and physical bondings.[228] Thus, the strong interaction can enhance the mechanical strength and operational durability of the GO membranes. Moreover, the strategy could apply to the enhancement of interconnection between GO nanosheets (Figure 12D). In a similar principle, the molecular bridge can form strong bonding adjacent to GO sheets, preventing severe swelling under aqueous conditions. Another approach without additives is thermal welding of the substrate. Specifically, polymeric supports can be easily melted by thermal treatment, which highly enhances adhesion between graphene and the supports.[57]

4.3. Membrane Fouling and Graphene Layer Compaction during Operation

Membrane fouling represents one of the most significant challenges in membrane applications for water treatment. The fouling refers to the undesired accumulation of substances including organic compounds, inorganic precipitates, and biological entities on the membrane surface or within its pores, leading to the deterioration of membrane performance.[229−231] GO-based membranes normally exhibit negatively charged properties due to abundant oxygen-containing groups.[18,232] The properties cause heavy solute accumulation, for charged solutes (e.g., dyes), on the membrane surface during long-term filtration, forming severe cake films as shown in Figure 13A.[57,151,233] The thick cake film leads to a significant flux decline by a longer diffusion length. Moreover, the effective solute concentration on the feed side of the membrane surface considerably increased due to solute accumulation. This phenomenon, known as concentration polarization, leads to decreased apparent rejection rates.[51,234−236]

In addition, the interlayers of GO membranes are possibly compacted under pressure, leading to a more ordered microstructure (Figure 13B).[237] The ordered structure of GO results in considerably reduced water flux during long-term filtration even though solute rejection rates increase.[81,237] The significant decline in the flux of GO membranes is one of the major challenges that must be addressed in practical membrane operations. In addition, because module operation has been rarely reported, it is not clear yet how the operation conditions of the module (e.g., flow rate, pressure, configuration of membrane) can affect the overall performance of the graphene-based membrane separation systems.

5. CONCLUSIONS

We reviewed recent research on graphene-based membranes for water treatment applications such as wastewater treatment, desalination, and ion recovery. Graphene can offer possibilities for versatile separation including water treatment due to its precise molecular sieving by the well-defined interlayer structure, which has been widely demonstrated and realized. Moreover, graphene could outperform existing polymeric membranes by modifying the pore, interlayer, or surface structure. In addition, scalable fabrication of graphene membranes, especially GO, has been recently attempted due to its viscoelastic properties and showed feasibility. Nonetheless, graphene-based membranes have not been commercialized for industrial scale since the development of graphene fabrication a decade ago. The molecular transport of graphene membranes has been intensively investigated and evaluated; therefore, research on graphene membranes should now focus on a realistic operation with module system development. We aimed for this review to provide a clear and comprehensive overview of graphene-based membranes and current issues in water-related environmental applications such as desalination, water extraction, and resource recovery. Furthermore, we discuss the challenges that need to be addressed to develop commercially viable graphene membranes. We hope this review serves as a basis for future research efforts aimed at overcoming these challenges and advancing the practical implementation of graphene-based membranes in large-scale water treatment systems.

AUTHOR INFORMATION

Corresponding Author

Dae Woo Kim − *Department of Chemical and Biomolecular Engineering, Yonsei University, Seodaemun-gu, Seoul 03722, Republic of Korea;* orcid.org/0000-0001-6533-8086; Email: audw1105@yonsei.ac.kr

Authors

Junhyeok Kang − *Department of Chemical and Biomolecular Engineering, Yonsei University, Seodaemun-gu, Seoul 03722, Republic of Korea*

Ohchan Kwon − *Department of Chemistry, University of California Berkeley, Berkeley, California 94720, United States*

Jeong Pil Kim − *Department of Chemical and Biomolecular Engineering, Yonsei University, Seodaemun-gu, Seoul 03722, Republic of Korea*

Ju Yeon Kim − *Department of Chemical and Biomolecular Engineering, Yonsei University, Seodaemun-gu, Seoul 03722, Republic of Korea*

Jiwon Kim − *Department of Chemical and Biomolecular Engineering, Yonsei University, Seodaemun-gu, Seoul 03722, Republic of Korea*

Yonghwi Cho − *Department of Chemical and Biomolecular Engineering, Yonsei University, Seodaemun-gu, Seoul 03722, Republic of Korea*

Complete contact information is available at: https://pubs.acs.org/10.1021/acsenvironau.4c00088

Author Contributions

[§]J.K. and O.K. contributed equally to this work. Credit: **Junhyeok Kang** Writing-original draft, Resources, Visualization, Validation; **Ohchan Kwon** Writing-original draft, Resources, Visualization, Validation; **Jeong Pil Kim** Writing-original draft, Visualization; **Ju Yeon Kim** Writing-original draft, Visualization; **Jiwon Kim**; Writing-original draft, Visualization; **Yonghwi Cho** Data curation; **Dae Woo Kim** Writing-original draft, Conceptualization, Funding acquisition, Supervision, Writing-review and editing.

Notes

The authors declare no competing financial interest.

ACKNOWLEDGMENTS

This reseach was supported by basic science research program through the National Research Foundation of Korea funded by the Ministry of Education (NRF-2019R1A6A1A11055660). This work was supported by the Industrial Strategic Technology Development Program ("Development of deuterium oxide localization and deuterium benzene synthesis technology to improve OLED lifetime by 25%", "20022479") funded by the Ministry of Trade, Industry & Energy (MOTIE, Korea). This work was supported by the Technology Innovation Program ("20013621", Center for Super Critical Material Industrial Technology) funded By the Ministry of Trade, Industry & Energy (MOTIE, Korea).

■ REFERENCES

(1) Mekonnen, M. M.; Hoekstra, A. Y. Four billion people facing severe water scarcity. *Sci. Adv.* **2016**, *2* (2), No. e1500323.

(2) He, C.; Liu, Z.; Wu, J.; Pan, X.; Fang, Z.; Li, J.; Bryan, B. A. Future global urban water scarcity and potential solutions. *Nat. Commun.* **2021**, *12* (1), 4667.

(3) Sim, J.; Lee, J.; Rho, H.; Park, K.-D.; Choi, Y.; Kim, D.; Kim, H.; Woo, Y. C. A review of semiconductor wastewater treatment processes: Current status, challenges, and future trends. *J. Clean Prod.* **2023**, *429*, No. 139570.

(4) Lee, H.; Jin, Y.; Hong, S. Recent transitions in ultrapure water (UPW) technology: Rising role of reverse osmosis (RO). *Desalination* **2016**, *399*, 185−197.

(5) Khan, M.; Al-Attas, T.; Roy, S.; Rahman, M. M.; Ghaffour, N.; Thangadurai, V.; Larter, S.; Hu, J.; Ajayan, P. M.; Kibria, M. G. Seawater electrolysis for hydrogen production: a solution looking for a problem? *Energy Environ. Sci.* **2021**, *14* (9), 4831−4839.

(6) Yang, Y.; Okonkwo, E. G.; Huang, G.; Xu, S.; Sun, W.; He, Y. On the sustainability of lithium ion battery industry−A review and perspective. *Energy Storage Mater.* **2021**, *36*, 186−212.

(7) Sholl, D. S.; Lively, R. P. Seven chemical separations to change the world. *Nature* **2016**, *532* (7600), 435−437.

(8) Shah, K. M.; Billinge, I. H.; Chen, X.; Fan, H.; Huang, Y.; Winton, R. K.; Yip, N. Y. Drivers, challenges, and emerging technologies for desalination of high-salinity brines: A critical review. *Desalination* **2022**, *538*, No. 115827.

(9) Kwon, O.; Choi, Y.; Kang, J.; Kim, J. H.; Choi, E.; Woo, Y. C.; Kim, D. W. A comprehensive review of MXene-based water-treatment membranes and technologies: Recent progress and perspectives. *Desalination* **2022**, *522*, No. 115448.

(10) Nie, L.; Chuah, C. Y.; Bae, T. H.; Lee, J. M. Graphene-based advanced membrane applications in organic solvent nanofiltration. *Adv. Funct. Mater.* **2021**, *31* (6), No. 2006949.

(11) Han, Y.; Xu, Z.; Gao, C. Ultrathin graphene nanofiltration membrane for water purification. *Adv. Funct. Mater.* **2013**, *23* (29), 3693−3700.

(12) Kang, K. M.; Kim, D. W.; Ren, C. E.; Cho, K. M.; Kim, S. J.; Choi, J. H.; Nam, Y. T.; Gogotsi, Y.; Jung, H.-T. Selective molecular separation on Ti3C2T x−graphene oxide membranes during pressure-driven filtration: comparison with graphene oxide and MXenes. *ACS Appl. Mater. Interfaces* **2017**, *9* (51), 44687−44694.

(13) Hirunpinyopas, W.; Prestat, E.; Worrall, S. D.; Haigh, S. J.; Dryfe, R. A.; Bissett, M. A. Desalination and nanofiltration through functionalized laminar MoS2 membranes. *ACS Nano* **2017**, *11* (11), 11082−11090.

(14) Cong, S.; Yuan, Y.; Wang, J.; Wang, Z.; Kapteijn, F.; Liu, X. Highly water-permeable metal−organic framework MOF-303 membranes for desalination. *J. Am. Chem. Soc.* **2021**, *143* (48), 20055−20058.

(15) Kwon, O.; Kim, M.; Choi, E.; Bae, J. H.; Yoo, S.; Won, J. C.; Kim, Y. H.; Shin, J. H.; Lee, J. S.; Kim, D. W. High−aspect ratio zeolitic imidazolate framework (ZIF) nanoplates for hydrocarbon separation membranes. *Sci. Adv.* **2022**, *8* (1), No. eabl6841.

(16) Shi, X.; Zhang, Z.; Yin, C.; Zhang, X.; Long, J.; Zhang, Z.; Wang, Y. Design of Three-Dimensional Covalent Organic Framework Membranes for Fast and Robust Organic Solvent Nanofiltration. *Angew. Chem.* **2022**, *134* (36), No. e202207559.

(17) Eum, K.; Kim, D. W.; Choi, Y.; Duan, X.; Hillmyer, M. A.; Tsapatsis, M. Assembly of graphene oxide nanosheets on diamine-treated PVDF hollow fiber as nanofiltration membranes. *ACS Appl. Polym. Mater.* **2020**, *2* (9), 3859−3866.

(18) Kang, J.; Choi, Y.; Kim, J. H.; Choi, E.; Choi, S. E.; Kwon, O.; Kim, D. W. Functionalized nanoporous graphene membrane with ultrafast and stable nanofiltration. *J. Membr. Sci.* **2021**, *618*, No. 118635.

(19) Chen, L.; Li, N.; Wen, Z.; Zhang, L.; Chen, Q.; Chen, L.; Si, P.; Feng, J.; Li, Y.; Lou, J.; et al. Graphene oxide based membrane intercalated by nanoparticles for high performance nanofiltration application. *Chem. Eng. J.* **2018**, *347*, 12−18.

(20) Wang, X.-Y.; Narita, A.; Müllen, K. Precision synthesis versus bulk-scale fabrication of graphenes. *Nat. Rev. Chem.* **2018**, *2* (1), 0100.

(21) Kim, D. W.; Choi, J.; Kim, D.; Jung, H.-T. Enhanced water permeation based on nanoporous multilayer graphene membranes: the role of pore size and density. *J. Mater. Chem. A* **2016**, *4* (45), 17773−17781.

(22) Choi, Y.; Kang, J.; Choi, E.; Kim, J. Y.; Kim, J. P.; Kim, J. H.; Kwon, O.; Kim, D. W. Carbon nanotube-supported graphene oxide nanoribbon bilayer membrane for high-performance diafiltration. *Chem. Eng. J.* **2022**, *427*, No. 131805.

(23) Li, Y.; Zhao, W.; Weyland, M.; Yuan, S.; Xia, Y.; Liu, H.; Jian, M.; Yang, J.; Easton, C. D.; Selomulya, C.; et al. Thermally reduced nanoporous graphene oxide membrane for desalination. *Environ. Sci. Technol.* **2019**, *53* (14), 8314−8323.

(24) Zhao, Z.; Ni, S.; Su, X.; Gao, Y.; Sun, X. Thermally reduced graphene oxide membrane with ultrahigh rejection of metal ions' separation from water. *ACS Sustain. Chem. Eng.* **2019**, *7* (17), 14874−14882.

(25) Kim, J. P.; Go, C. Y.; Kang, J.; Choi, Y.; Kim, J. Y.; Kim, J.; Kwon, O.; Kim, K. C.; Kim, D. W. Nanoporous multilayer graphene oxide membrane for forward osmosis metal ion recovery from spent Li-ion batteries. *J. Membr. Sci.* **2023**, *676*, No. 121590.

(26) Kim, J. H.; Choi, Y.; Kang, J.; Choi, E.; Choi, S. E.; Kwon, O.; Kim, D. W. Scalable fabrication of deoxygenated graphene oxide nanofiltration membrane by continuous slot-die coating. *J. Membr. Sci.* **2020**, *612*, No. 118454.

(27) Kwon, O.; Choi, Y.; Choi, E.; Kim, M.; Woo, Y. C.; Kim, D. W. Fabrication techniques for graphene oxide-based molecular separation membranes: Towards industrial application. *Nanomaterials* **2021**, *11* (3), 757.

(28) Yang, E.; Karahan, H. E.; Goh, K.; Chuah, C. Y.; Wang, R.; Bae, T.-H. Scalable fabrication of graphene-based laminate membranes for liquid and gas separations by crosslinking-induced gelation and doctor-blade casting. *Carbon* **2019**, *155*, 129−137.

(29) Esfahani, A. R.; Ma, C.; Flewellen, U. A.; Nair, S.; Harris, T. A. Scalable aqueous-phase fabrication of reduced graphene oxide nanofiltration membranes by an integrated roll-to-roll (R2R) process. *J. Membr. Sci.* **2023**, *678*, No. 121669.

(30) Kumari, P.; Tripathi, K. M.; Jangir, L. K.; Gupta, R.; Awasthi, K. Recent advances in application of the graphene-based membrane for water purification. *Mater. Today Chem.* **2021**, *22*, No. 100597.

(31) Tiwary, S. K.; Singh, M.; Chavan, S. V.; Karim, A. Graphene oxide-based membranes for water desalination and purification. *npj 2D Mater. Appl.* **2024**, *8* (1), 27.

(32) Alkhouzaam, A.; Qiblawey, H. Functional GO-based membranes for water treatment and desalination: Fabrication methods, performance and advantages. A review. *Chemosphere* **2021**, *274*, No. 129853.

(33) Chong, J.; Wang, B.; Li, K. Water transport through graphene oxide membranes: the roles of driving forces. *Chem. Commun.* **2018**, *54* (20), 2554−2557.

(34) Mi, B. Graphene oxide membranes for ionic and molecular sieving. *Science* **2014**, *343* (6172), 740−742.

(35) Zheng, S.; Tu, Q.; Urban, J. J.; Li, S.; Mi, B. Swelling of graphene oxide membranes in aqueous solution: characterization of interlayer spacing and insight into water transport mechanisms. *ACS Nano* **2017**, *11* (6), 6440−6450.

(36) Joshi, R.; Carbone, P.; Wang, F.-C.; Kravets, V. G.; Su, Y.; Grigorieva, I. V.; Wu, H.; Geim, A. K.; Nair, R. R. Precise and ultrafast molecular sieving through graphene oxide membranes. *science* **2014**, *343* (6172), 752−754.

(37) Kang, J.; Ko, Y.; Kim, J. P.; Kim, J. Y.; Kim, J.; Kwon, O.; Kim, K. C.; Kim, D. W. Microwave-assisted design of nanoporous graphene membrane for ultrafast and switchable organic solvent nanofiltration. *Nat. Commun.* **2023**, *14* (1), 901.

(38) Nair, R.; Wu, H.; Jayaram, P. N.; Grigorieva, I. V.; Geim, A. Unimpeded permeation of water through helium-leak−tight graphene-based membranes. *Science* **2012**, *335* (6067), 442−444.

(39) Cao, Y.; Xiong, Z.; Xia, F.; Franks, G. V.; Zu, L.; Wang, X.; Hora, Y.; Mudie, S.; He, Z.; Qu, L.; et al. New structural insights into densely assembled reduced graphene oxide membranes. *Adv. Funct. Mater.* **2022**, *32* (42), No. 2201535.
(40) Qi, B.; He, X.; Zeng, G.; Pan, Y.; Li, G.; Liu, G.; Zhang, Y.; Chen, W.; Sun, Y. Strict molecular sieving over electrodeposited 2D-interspacing-narrowed graphene oxide membranes. *Nat. Commun.* **2017**, *8* (1), 825.
(41) Wei, N.; Peng, X.; Xu, Z. Understanding water permeation in graphene oxide membranes. *ACS Appl. Mater. Interfaces* **2014**, *6* (8), 5877−5883.
(42) Yu, H.; He, Y.; Xiao, G.; Fan, Y.; Ma, J.; Gao, Y.; Hou, R.; Yin, X.; Wang, Y.; Mei, X. The roles of oxygen-containing functional groups in modulating water purification performance of graphene oxide-based membrane. *Chem. Eng. J.* **2020**, *389*, No. 124375.
(43) Xing, Y.-L.; Xu, G.-R.; An, Z.-H.; Liu, Y.-H.; Xu, K.; Liu, Q.; Zhao, H.-L.; Das, R. Laminated GO membranes for water transport and ions selectivity: Mechanism, synthesis, stabilization, and applications. *Sep. Purif. Technol.* **2021**, *259*, No. 118192.
(44) Kim, D. W.; Jang, J.; Kim, I.; Nam, Y. T.; Jung, Y.; Jung, H.-T. Revealing the role of oxygen debris and functional groups on the water flux and molecular separation of graphene oxide membrane: a combined experimental and theoretical study. *J. Phys. Chem. C* **2018**, *122* (30), 17507−17517.
(45) Qiu, R.; Yuan, S.; Xiao, J.; Chen, X. D.; Selomulya, C.; Zhang, X.; Woo, M. W. Effects of edge functional groups on water transport in graphene oxide membranes. *ACS Appl. Mater. Interfaces* **2019**, *11* (8), 8483−8491.
(46) Zhang, M.; Guan, K.; Ji, Y.; Liu, G.; Jin, W.; Xu, N. Controllable ion transport by surface-charged graphene oxide membrane. *Nat. Commun.* **2019**, *10* (1), 1253.
(47) Dimiev, A. M.; Alemany, L. B.; Tour, J. M. Graphene oxide. Origin of acidity, its instability in water, and a new dynamic structural model. *ACS Nano* **2013**, *7* (1), 576−588.
(48) Huang, H.; Mao, Y.; Ying, Y.; Liu, Y.; Sun, L.; Peng, X. Salt concentration, pH and pressure controlled separation of small molecules through lamellar graphene oxide membranes. *Chem. Commun.* **2013**, *49* (53), 5963−5965.
(49) Sun, P.; Zhu, M.; Wang, K.; Zhong, M.; Wei, J.; Wu, D.; Xu, Z.; Zhu, H. Selective ion penetration of graphene oxide membranes. *ACS Nano* **2013**, *7* (1), 428−437.
(50) Wen, X.; Foller, T.; Jin, X.; Musso, T.; Kumar, P.; Joshi, R. Understanding water transport through graphene-based nanochannels via experimental control of slip length. *Nat. Commun.* **2022**, *13* (1), 5690.
(51) Nie, L.; Goh, K.; Wang, Y.; Lee, J.; Huang, Y.; Karahan, H. E.; Zhou, K.; Guiver, M. D.; Bae, T.-H. Realizing small-flake graphene oxide membranes for ultrafast size-dependent organic solvent nanofiltration. *Sci. Adv.* **2020**, *6* (17), No. eaaz9184.
(52) Muscatello, J.; Jaeger, F.; Matar, O. K.; Müller, E. A. Optimizing water transport through graphene-based membranes: insights from nonequilibrium molecular dynamics. *ACS Appl. Mater. Interfaces* **2016**, *8* (19), 12330−12336.
(53) Kim, T.-N.; Lee, J.-M.; Park, S.-G.; Lee, J.; Yang, E.; Hwang, M.-H.; Goh, K.; Chae, K.-J. Size-dependent water transport in laminar graphene oxide membranes: An interplay between interlayer spacing versus tortuosity of transport pathway. *Carbon* **2024**, *216*, No. 118560.
(54) Lin, L.-C.; Grossman, J. C. Atomistic understandings of reduced graphene oxide as an ultrathin-film nanoporous membrane for separations. *Nat. Commun.* **2015**, *6* (1), 8335.
(55) Xu, Y.; Chen, C.-Y.; Zhao, Z.; Lin, Z.; Lee, C.; Xu, X.; Wang, C.; Huang, Y.; Shakir, M. I.; Duan, X. Solution processable holey graphene oxide and its derived macrostructures for high-performance supercapacitors. *Nano Lett.* **2015**, *15* (7), 4605−4610.
(56) Kang, J.; Choi, Y.; Kim, J. P.; Kim, J. H.; Kim, J. Y.; Kwon, O.; Kim, D. I.; Kim, D. W. Thermally-induced pore size tuning of multilayer nanoporous graphene for organic solvent nanofiltration. *J. Membr. Sci.* **2021**, *637*, No. 119620.
(57) Kim, J.; Kang, J.; Kim, J. P.; Kim, J. Y.; Kim, J. H.; Kwon, O.; Kim, D. W. Scalable fabrication of nanoporous multilayer graphene oxide membrane for organic solvent nanofiltration. *Carbon* **2023**, *207*, 162−171.
(58) Suk, M. E.; Aluru, N. R. Water transport through ultrathin graphene. *J. Phys. Chem. Lett.* **2010**, *1* (10), 1590−1594.
(59) Cohen-Tanugi, D.; Grossman, J. C. Water desalination across nanoporous graphene. *Nano Lett.* **2012**, *12* (7), 3602−3608.
(60) Hummers, W. S., Jr; Offeman, R. E. Preparation of graphitic oxide. *J. Am. Chem. Soc.* **1958**, *80* (6), 1339−1339.
(61) Marcano, D. C.; Kosynkin, D. V.; Berlin, J. M.; Sinitskii, A.; Sun, Z.; Slesarev, A.; Alemany, L. B.; Lu, W.; Tour, J. M. Improved synthesis of graphene oxide. *ACS Nano* **2010**, *4* (8), 4806−4814.
(62) Dimiev, A. M.; Tour, J. M. Mechanism of graphene oxide formation. *ACS Nano* **2014**, *8* (3), 3060−3068.
(63) Dikin, D. A.; Stankovich, S.; Zimney, E. J.; Piner, R. D.; Dommett, G. H.; Evmenenko, G.; Nguyen, S. T.; Ruoff, R. S. Preparation and characterization of graphene oxide paper. *Nature* **2007**, *448* (7152), 457−460.
(64) Tsou, C.-H.; An, Q.-F.; Lo, S.-C.; De Guzman, M.; Hung, W.-S.; Hu, C.-C.; Lee, K.-R.; Lai, J.-Y. Effect of microstructure of graphene oxide fabricated through different self-assembly techniques on 1-butanol dehydration. *J. Membr. Sci.* **2015**, *477*, 93−100.
(65) Shen, J.; Liu, G.; Huang, K.; Chu, Z.; Jin, W.; Xu, N. Subnanometer two-dimensional graphene oxide channels for ultrafast gas sieving. *ACS Nano* **2016**, *10* (3), 3398−3409.
(66) Zhang, Y.; Shen, Q.; Hou, J.; Sutrisna, P. D.; Chen, V. Shear-aligned graphene oxide laminate/Pebax ultrathin composite hollow fiber membranes using a facile dip-coating approach. *J. Mater. Chem. A* **2017**, *5* (17), 7732−7737.
(67) Akbari, A.; Sheath, P.; Martin, S. T.; Shinde, D. B.; Shaibani, M.; Banerjee, P. C.; Tkacz, R.; Bhattacharyya, D.; Majumder, M. Large-area graphene-based nanofiltration membranes by shear alignment of discotic nematic liquid crystals of graphene oxide. *Nat. Commun.* **2016**, *7* (1), 10891.
(68) Choi, S. E.; Kim, S.-S.; Choi, E.; Kim, J. H.; Choi, Y.; Kang, J.; Kwon, O.; Kim, D. W. Diamine vapor treatment of viscoelastic graphene oxide liquid crystal for gas barrier coating. *Sci. Rep.* **2021**, *11* (1), 9518.
(69) Kim, J. H.; Choi, Y.; Kang, J.; Kim, J. Y.; Bae, J. H.; Kwon, O.; Kim, D. W. Shear-induced assembly of high-aspect-ratio graphene nanoribbon nanosheets in a confined microchannel: Membrane fabrication for ultrafast organic solvent nanofiltration. *Carbon* **2022**, *191*, 563−570.
(70) Kwon, Y. A.; Kim, J.; Jo, S. B.; Roe, D. G.; Rhee, D.; Song, Y.; Kang, B.; Kim, D.; Kim, J.; Kim, D. W.; et al. Wafer-scale transistor arrays fabricated using slot-die printing of molybdenum disulfide and sodium-embedded alumina. *Nat. Electron.* **2023**, *6* (6), 443−450.
(71) Kim, J. H.; Park, G. S.; Kim, Y.-J.; Choi, E.; Kang, J.; Kwon, O.; Kim, S. J.; Cho, J. H.; Kim, D. W. Large-Area Ti3C2T x-MXene coating: toward industrial-scale fabrication and molecular separation. *ACS Nano* **2021**, *15* (5), 8860−8869.
(72) Liu, Z.; Ma, Z.; Qian, B.; Chan, A. Y.; Wang, X.; Liu, Y.; Xin, J. H. A facile and scalable method of fabrication of large-area ultrathin graphene oxide nanofiltration membrane. *ACS Nano* **2021**, *15* (9), 15294−15305.
(73) Liu, Z.; Ma, Z.; Wang, X.; Ye, D.; Yu, H.; Xin, J. H. Ultrathin graphene oxide membrane for pilot scale dyehouse effluent treatment. *Desalination* **2022**, *537*, No. 115876.
(74) Shenvi, S. S.; Isloor, A. M.; Ismail, A. A review on RO membrane technology: Developments and challenges. *Desalination* **2015**, *368*, 10−26.
(75) Hailemariam, R. H.; Woo, Y. C.; Damtie, M. M.; Kim, B. C.; Park, K.-D.; Choi, J.-S. Reverse osmosis membrane fabrication and modification technologies and future trends: A review. *Adv. Colloid Interface Sci.* **2020**, *276*, No. 102100.
(76) Ritt, C. L.; Stassin, T.; Davenport, D. M.; DuChanois, R. M.; Nulens, I.; Yang, Z.; Ben-Zvi, A.; Segev-Mark, N.; Elimelech, M.; Tang, C. Y.; et al. The open membrane database: Synthesis−

structure−performance relationships of reverse osmosis membranes. *J. Membr. Sci.* **2022**, *641*, No. 119927.

(77) Verbeke, R.; Gomez, V.; Vankelecom, I. F. Chlorine-resistance of reverse osmosis (RO) polyamide membranes. *Prog. Polym. Sci.* **2017**, *72*, 1−15.

(78) Luque-Alled, J. M.; Martínez-Izquierdo, L.; Gorgojo, P.; Téllez, C.; Coronas, J. Organic solvent-free fabrication of thin film polyamide/zeolitic imidazolate framework membranes for removal of dyes from water. *Chem. Eng. J.* **2023**, *470*, No. 144233.

(79) Prat, D.; Hayler, J.; Wells, A. A survey of solvent selection guides. *Green Chem.* **2014**, *16* (10), 4546−4551.

(80) Chen, L.; Shi, G.; Shen, J.; Peng, B.; Zhang, B.; Wang, Y.; Bian, F.; Wang, J.; Li, D.; Qian, Z.; et al. Ion sieving in graphene oxide membranes via cationic control of interlayer spacing. *Nature* **2017**, *550* (7676), 380−383.

(81) Li, W.; Wu, W.; Li, Z. Controlling interlayer spacing of graphene oxide membranes by external pressure regulation. *ACS Nano* **2018**, *12* (9), 9309−9317.

(82) Wang, Z.; Ma, C.; Xu, C.; Sinquefield, S. A.; Shofner, M. L.; Nair, S. Graphene oxide nanofiltration membranes for desalination under realistic conditions. *Nat. Sustain.* **2021**, *4* (5), 402−408.

(83) Guan, K.; Mai, Z.; Zhou, S.; Fang, S.; Li, Z.; Xu, P.; Chiao, Y.-H.; Hu, M.; Zhang, P.; Xu, G.; et al. Side-Chain-Dependent Functional Intercalations in Graphene Oxide Membranes for Selective Water and Ion Transport. *Nano Lett.* **2023**, *23* (13), 6095−6101.

(84) Ahmed, M. A.; Mahmoud, S. A.; Mohamed, A. A. Nanomaterials-modified reverse osmosis membranes: a comprehensive review. *RSC Adv.* **2024**, *14* (27), 18879−18906.

(85) Wang, C.; Park, M. J.; Seo, D. H.; Shon, H. K. Inkjet printing of graphene oxide and dopamine on nanofiltration membranes for improved anti-fouling properties and chlorine resistance. *Sep. Purif. Technol.* **2021**, *254*, No. 117604.

(86) Wang, C.; Tian, W.; Wei, Y.; Li, X.; Zhang, Q.; Huang, C. Study on the association between residential exposure to N, N-dimethylformamide and hospitalization for respiratory disease. *Atmos. Environ.* **2013**, *77*, 166−171.

(87) Naziri Mehrabani, S. A.; Vatanpour, V.; Koyuncu, I. Green solvents in polymeric membrane fabrication: A review. *Sep. Purif. Technol.* **2022**, *298*, No. 121691.

(88) Hung, W.-S.; Tsou, C.-H.; De Guzman, M.; An, Q.-F.; Liu, Y.-L.; Zhang, Y.-M.; Hu, C.-C.; Lee, K.-R.; Lai, J.-Y. Cross-linking with diamine monomers to prepare composite graphene oxide-framework membranes with varying d-spacing. *Chem. Mater.* **2014**, *26* (9), 2983−2990.

(89) Kim, S.; Ou, R.; Hu, Y.; Li, X.; Zhang, H.; Simon, G. P.; Wang, H. Non-swelling graphene oxide-polymer nanocomposite membrane for reverse osmosis desalination. *J. Membr. Sci.* **2018**, *562*, 47−55.

(90) Yang, Z.; Guo, H.; Tang, C. Y. The upper bound of thin-film composite (TFC) polyamide membranes for desalination. *J. Membr. Sci.* **2019**, *590*, No. 117297.

(91) Lu, X.; Elimelech, M. Fabrication of desalination membranes by interfacial polymerization: history, current efforts, and future directions. *Chem. Soc. Rev.* **2021**, *50* (11), 6290−6307.

(92) Hung, W.-S.; Lin, T.-J.; Chiao, Y.-H.; Sengupta, A.; Hsiao, Y.-C.; Wickramasinghe, S. R.; Hu, C.-C.; Lee, K.-R.; Lai, J.-Y. Graphene-induced tuning of the d-spacing of graphene oxide composite nanofiltration membranes for frictionless capillary action-induced enhancement of water permeability. *J. Mater. Chem. A* **2018**, *6* (40), 19445−19454.

(93) Guan, K.; Jia, Y.; Lin, Y.; Wang, S.; Matsuyama, H. Chemically converted graphene nanosheets for the construction of ion-exclusion nanochannel membranes. *Nano Lett.* **2021**, *21* (8), 3495−3502.

(94) Yang, Q.; Su, Y.; Chi, C.; Cherian, C.; Huang, K.; Kravets, V.; Wang, F.; Zhang, J.; Pratt, A.; Grigorenko, A.; et al. Ultrathin graphene-based membrane with precise molecular sieving and ultrafast solvent permeation. *Nat. Mater.* **2017**, *16* (12), 1198−1202.

(95) Yuan, S.; Li, Y.; Xia, Y.; Selomulya, C.; Zhang, X. Stable cation-controlled reduced graphene oxide membranes for improved NaCl rejection. *J. Membr. Sci.* **2021**, *621*, No. 118995.

(96) Xu, X.-L.; Lin, F.-W.; Du, Y.; Zhang, X.; Wu, J.; Xu, Z.-K. Graphene oxide nanofiltration membranes stabilized by cationic porphyrin for high salt rejection. *ACS Appl. Mater. Interfaces* **2016**, *8* (20), 12588−12593.

(97) Chen, X.; Qiu, M.; Ding, H.; Fu, K.; Fan, Y. A reduced graphene oxide nanofiltration membrane intercalated by well-dispersed carbon nanotubes for drinking water purification. *Nanoscale* **2016**, *8* (10), 5696−5705.

(98) Morelos-Gomez, A.; Cruz-Silva, R.; Muramatsu, H.; Ortiz-Medina, J.; Araki, T.; Fukuyo, T.; Tejima, S.; Takeuchi, K.; Hayashi, T.; Terrones, M.; et al. Effective NaCl and dye rejection of hybrid graphene oxide/graphene layered membranes. *Nat. Nanotechnol.* **2017**, *12* (11), 1083−1088.

(99) Yang, Y.; Yang, X.; Liang, L.; Gao, Y.; Cheng, H.; Li, X.; Zou, M.; Ma, R.; Yuan, Q.; Duan, X. Large-area graphene-nanomesh/carbon-nanotube hybrid membranes for ionic and molecular nanofiltration. *Science* **2019**, *364* (6445), 1057−1062.

(100) Abraham, J.; Vasu, K. S.; Williams, C. D.; Gopinadhan, K.; Su, Y.; Cherian, C. T.; Dix, J.; Prestat, E.; Haigh, S. J.; Grigorieva, I. V.; et al. Tunable sieving of ions using graphene oxide membranes. *Nat. Nanotechnol.* **2017**, *12* (6), 546−550.

(101) Wang, L.; Yuan, Z.; Zhang, Y.; Guo, W.; Sun, X.; Duan, X. Sandwich layered double hydroxides with graphene oxide for enhanced water desalination. *Sci. China Mater.* **2022**, *65* (3), 803−810.

(102) Qian, Y.; Shang, J.; Liu, D.; Yang, G.; Wang, X.; Chen, C.; Kou, L.; Lei, W. Enhanced ion sieving of graphene oxide membranes via surface amine functionalization. *J. Am. Chem. Soc.* **2021**, *143* (13), 5080−5090.

(103) Pang, J.; Kang, Z.; Wang, R.; Xu, B.; Nie, X.; Fan, L.; Zhang, F.; Du, X.; Feng, S.; Sun, D. Exploring the sandwich antibacterial membranes based on UiO-66/graphene oxide for forward osmosis performance. *Carbon* **2019**, *144*, 321−332.

(104) Guan, K.; Guo, Y.; Li, Z.; Jia, Y.; Shen, Q.; Nakagawa, K.; Yoshioka, T.; Liu, G.; Jin, W.; Matsuyama, H. Deformation constraints of graphene oxide nanochannels under reverse osmosis. *Nat. Commun.* **2023**, *14* (1), 1016.

(105) Achilli, A.; Cath, T. Y.; Childress, A. E. Selection of inorganic-based draw solutions for forward osmosis applications. *J. Membr. Sci.* **2010**, *364* (1−2), 233−241.

(106) Zhao, S.; Zou, L.; Mulcahy, D. Brackish water desalination by a hybrid forward osmosis−nanofiltration system using divalent draw solute. *Desalination* **2012**, *284*, 175−181.

(107) Ge, Q.; Su, J.; Amy, G. L.; Chung, T.-S. Exploration of polyelectrolytes as draw solutes in forward osmosis processes. *Water Res.* **2012**, *46* (4), 1318−1326.

(108) Ge, Q.; Wang, P.; Wan, C.; Chung, T.-S. Polyelectrolyte-promoted forward osmosis−membrane distillation (FO−MD) hybrid process for dye wastewater treatment. *Environ. Sci. Technol.* **2012**, *46* (11), 6236−6243.

(109) Arcanjo, G. S.; Costa, F. C.; Ricci, B. C.; Mounteer, A. H.; de Melo, E. N.; Cavalcante, B. F.; Araújo, A. V.; Faria, C. V.; Amaral, M. C. Draw solution solute selection for a hybrid forward osmosis-membrane distillation module: effects on trace organic compound rejection, water flux and polarization. *Chem. Eng. J.* **2020**, *400*, No. 125857.

(110) Liu, S.; Tong, X.; Chen, Y.; Crittenden, J. Forward solute transport in forward osmosis using a freestanding graphene oxide membrane. *Environ. Sci. Technol.* **2021**, *55* (9), 6290−6298.

(111) Yang, E.; Kim, C.-M.; Song, J.-h.; Ki, H.; Ham, M.-H.; Kim, I. S. Enhanced desalination performance of forward osmosis membranes based on reduced graphene oxide laminates coated with hydrophilic polydopamine. *Carbon* **2017**, *117*, 293−300.

(112) Huang, H.; Song, Z.; Wei, N.; Shi, L.; Mao, Y.; Ying, Y.; Sun, L.; Xu, Z.; Peng, X. Ultrafast viscous water flow through nanostrand-channelled graphene oxide membranes. *Nat. Commun.* **2013**, *4* (1), 2979.

(113) Liu, H.; Wang, H.; Zhang, X. Facile fabrication of freestanding ultrathin reduced graphene oxide membranes for water purification. *Adv. Mater.* **2015**, *27* (2), 249−254.
(114) Tong, X.; Wang, X.; Liu, S.; Gao, H.; Xu, C.; Crittenden, J.; Chen, Y. A freestanding graphene oxide membrane for efficiently harvesting salinity gradient power. *Carbon* **2018**, *138*, 410−418.
(115) Tong, X.; Liu, S.; Zhao, Y.; Xiao, C.; Chen, Y.; Crittenden, J. A freestanding graphene oxide framework membrane for forward osmosis: Separation performance and transport mechanistic insights. *J. Membr. Sci.* **2022**, *661*, No. 120919.
(116) Peng, W.; Escobar, I. C. Rejection efficiency of water quality parameters by reverse osmosis and nanofiltration membranes. *Environ. Sci. Technol.* **2003**, *37* (19), 4435−4441.
(117) Zhang, Y.; Chung, T.-S. Graphene oxide membranes for nanofiltration. *Curr. Opin. Chem. Eng.* **2017**, *16*, 9−15.
(118) Van der Bruggen, B.; Vandecasteele, C. Modelling of the retention of uncharged molecules with nanofiltration. *Water Res.* **2002**, *36* (5), 1360−1368.
(119) Tang, C. Y.; Chong, T.; Fane, A. G. Colloidal interactions and fouling of NF and RO membranes: a review. *Adv. Colloid Interface Sci.* **2011**, *164* (1−2), 126−143.
(120) Geim, A. K. Graphene: status and prospects. *Science* **2009**, *324* (5934), 1530−1534.
(121) Liu, G.; Jin, W.; Xu, N. Graphene-based membranes. *Chem. Soc. Rev.* **2015**, *44* (15), 5016−5030.
(122) Cho, K. M.; Lee, H.-J.; Nam, Y. T.; Kim, Y.-J.; Kim, C.; Kang, K. M.; Ruiz Torres, C. A.; Kim, D. W.; Jung, H.-T. Ultrafast-selective nanofiltration of an hybrid membrane comprising laminated reduced graphene oxide/graphene oxide nanoribbons. *ACS Appl. Mater. Interfaces* **2019**, *11* (30), 27004−27010.
(123) Qiu, L.; Zhang, X.; Yang, W.; Wang, Y.; Simon, G. P.; Li, D. Controllable corrugation of chemically converted graphene sheets in water and potential application for nanofiltration. *Chem. Commun.* **2011**, *47* (20), 5810−5812.
(124) Yeh, C.-N.; Raidongia, K.; Shao, J.; Yang, Q.-H.; Huang, J. On the origin of the stability of graphene oxide membranes in water. *Nat. Chem.* **2015**, *7* (2), 166−170.
(125) Nam, Y. T.; Choi, J.; Kang, K. M.; Kim, D. W.; Jung, H.-T. Enhanced stability of laminated graphene oxide membranes for nanofiltration via interstitial amide bonding. *ACS Appl. Mater. Interfaces* **2016**, *8* (40), 27376−27382.
(126) Thebo, K. H.; Qian, X.; Zhang, Q.; Chen, L.; Cheng, H.-M.; Ren, W. Highly stable graphene-oxide-based membranes with superior permeability. *Nat. Commun.* **2018**, *9* (1), 1486.
(127) Goh, K.; Jiang, W.; Karahan, H. E.; Zhai, S.; Wei, L.; Yu, D.; Fane, A. G.; Wang, R.; Chen, Y. All-carbon nanoarchitectures as high-performance separation membranes with superior stability. *Adv. Funct. Mater.* **2015**, *25* (47), 7348−7359.
(128) Ying, Y.; He, P.; Wei, M.; Ding, G.; Peng, X. Robust GQDs modified thermally reduced graphene oxide membranes for ultrafast and long-term purification of dye-wasted water. *Adv. Mater. Interfaces* **2017**, *4* (14), No. 1700209.
(129) Zambare, R. S.; Song, X.; Bhuvana, S.; Tang, C. Y.; Prince, J. A.; Nemade, P. R. Ionic liquid-reduced graphene oxide membrane with enhanced stability for water purification. *ACS Appl. Mater. Interfaces* **2022**, *14* (38), 43339−43353.
(130) Li, Y.; Yuan, S.; Xia, Y.; Zhao, W.; Easton, C. D.; Selomulya, C.; Zhang, X. Mild annealing reduced graphene oxide membrane for nanofiltration. *J. Membr. Sci.* **2020**, *601*, No. 117900.
(131) Jang, J.; Nam, Y. T.; Kim, D.; Kim, Y.-J.; Kim, D. W.; Jung, H.-T. Turbostratic nanoporous carbon sheet membrane for ultrafast and selective nanofiltration in viscous green solvents. *J. Mater. Chem. A* **2020**, *8* (17), 8292−8299.
(132) Wang, Z.; He, F.; Guo, J.; Peng, S.; Cheng, X. Q.; Zhang, Y.; Drioli, E.; Figoli, A.; Li, Y.; Shao, L. The stability of a graphene oxide (GO) nanofiltration (NF) membrane in an aqueous environment: Progress and challenges. *Mater. Adv.* **2020**, *1* (4), 554−568.
(133) Guan, K.; Zhao, D.; Zhang, M.; Shen, J.; Zhou, G.; Liu, G.; Jin, W. 3D nanoporous crystals enabled 2D channels in graphene membrane with enhanced water purification performance. *J. Membr. Sci.* **2017**, *542*, 41−51.
(134) Han, Y.; Jiang, Y.; Gao, C. High-flux graphene oxide nanofiltration membrane intercalated by carbon nanotubes. *ACS Appl. Mater. Interfaces* **2015**, *7* (15), 8147−8155.
(135) Cheng, M.-m.; Huang, L.-j.; Wang, Y.-x.; Tang, J.-g.; Wang, Y.; Zhao, Y.-c.; Liu, G.-f.; Zhang, Y.; Kipper, M. J.; Wickramasinghe, S. R. Reduced graphene oxide−gold nanoparticle membrane for water purification. *Sep. Sci. Technol.* **2019**, *54* (6), 1079−1085.
(136) Kim, J. Y.; Choi, Y.; Choi, J.; Kim, Y.-J.; Kang, J.; Kim, J. P.; Kim, J. H.; Kwon, O.; Kim, S.-S.; Kim, D. W. Graphene nanoribbon/carbon nanotube hybrid hydrogel: rheology and membrane for ultrafast molecular diafiltration. *ACS Appl. Mater. Interfaces* **2022**, *14* (9), 11779−11788.
(137) Xiong, R.; Kim, H. S.; Zhang, L.; Korolovych, V. F.; Zhang, S.; Yingling, Y. G.; Tsukruk, V. V. Wrapping nanocellulose nets around graphene oxide sheets. *Angew. Chem.-Int. Ed.* **2018**, *57* (28), 8508−8513.
(138) Celebi, K.; Buchheim, J.; Wyss, R. M.; Droudian, A.; Gasser, P.; Shorubalko, I.; Kye, J.-I.; Lee, C.; Park, H. G. Ultimate permeation across atomically thin porous graphene. *Science* **2014**, *344* (6181), 289−292.
(139) Surwade, S. P.; Smirnov, S. N.; Vlassiouk, I. V.; Unocic, R. R.; Veith, G. M.; Dai, S.; Mahurin, S. M. Water desalination using nanoporous single-layer graphene. *Nat. Nanotechnol.* **2015**, *10* (5), 459−464.
(140) Huh, S.; Park, J.; Kim, Y. S.; Kim, K. S.; Hong, B. H.; Nam, J.-M. UV/ozone-oxidized large-scale graphene platform with large chemical enhancement in surface-enhanced Raman scattering. *ACS Nano* **2011**, *5* (12), 9799−9806.
(141) Fan, Z.; Zhao, Q.; Li, T.; Yan, J.; Ren, Y.; Feng, J.; Wei, T. Easy synthesis of porous graphene nanosheets and their use in supercapacitors. *Carbon* **2012**, *50* (4), 1699−1703.
(142) Yu, J.; He, Y.; Wang, Y.; Li, S.; Tian, S. Ethylenediamine-oxidized sodium alginate hydrogel cross-linked graphene oxide nanofiltration membrane with self-healing property for efficient dye separation. *J. Membr. Sci.* **2023**, *670*, No. 121366.
(143) Huang, L.; Chen, J.; Gao, T.; Zhang, M.; Li, Y.; Dai, L.; Qu, L.; Shi, G. Reduced graphene oxide membranes for ultrafast organic solvent nanofiltration. *Adv. Mater.* **2016**, *28* (39), 8669−8674.
(144) Jang, J.-H.; Woo, J. Y.; Lee, J.; Han, C.-S. Ambivalent effect of thermal reduction in mass rejection through graphene oxide membrane. *Environ. Sci. Technol.* **2016**, *50* (18), 10024−10030.
(145) Chen, L.; Li, Y.; Chen, L.; Li, N.; Dong, C.; Chen, Q.; Liu, B.; Ai, Q.; Si, P.; Feng, J.; et al. A large-area free-standing graphene oxide multilayer membrane with high stability for nanofiltration applications. *Chem. Eng. J.* **2018**, *345*, 536−544.
(146) Choi, Y.; Kim, S.-S.; Kim, J. H.; Kang, J.; Choi, E.; Choi, S. E.; Kim, J. P.; Kwon, O.; Kim, D. W. Graphene oxide nanoribbon hydrogel: viscoelastic behavior and use as a molecular separation membrane. *ACS Nano* **2020**, *14* (9), 12195−12202.
(147) Ying, Y.; Sun, L.; Wang, Q.; Fan, Z.; Peng, X. In-plane mesoporous graphene oxide nanosheet assembled membranes for molecular separation. *RSC Adv.* **2014**, *4* (41), 21425−21428.
(148) Hu, M.; Mi, B. Enabling graphene oxide nanosheets as water separation membranes. *Environ. Sci. Technol.* **2013**, *47* (8), 3715−3723.
(149) Zhang, W.; Xu, H.; Xie, F.; Ma, X.; Niu, B.; Chen, M.; Zhang, H.; Zhang, Y.; Long, D. General synthesis of ultrafine metal oxide/reduced graphene oxide nanocomposites for ultrahigh-flux nanofiltration membrane. *Nat. Commun.* **2022**, *13* (1), 471.
(150) Gao, S. J.; Qin, H.; Liu, P.; Jin, J. SWCNT-intercalated GO ultrathin films for ultrafast separation of molecules. *J. Mater. Chem. A* **2015**, *3* (12), 6649−6654.
(151) Ruiz-Torres, C. A.; Kang, J.; Kang, K. M.; Cho, K. M.; Nam, Y. T.; Byon, C.; Chang, Y.-Y.; Kim, D. W.; Jung, H.-T. Graphene-based ultrafast nanofiltration membrane under cross-flow operation: Effect of high-flux and filtered solute on membrane performance. *Carbon* **2021**, *185*, 641−649.

(152) Tiwary, S. K.; Singh, M.; Likhi, F. H.; Dabade, S.; Douglas, J. F.; Karim, A. Self-cross-linking of MXene-intercalated graphene oxide membranes with antiswelling properties for dye and salt rejection. *ACS Environ. Au* **2024**, *4* (2), 69−79.
(153) Balti, R.; Zayoud, N.; Hubert, F.; Beaulieu, L.; Massé, A. Fractionation of Arthrospira platensis (Spirulina) water soluble proteins by membrane diafiltration. *Sep. Purif. Technol.* **2021**, *256*, No. 117756.
(154) Sheth, J. P.; Qin, Y.; Sirkar, K. K.; Baltzis, B. C. Nanofiltration-based diafiltration process for solvent exchange in pharmaceutical manufacturing. *J. Membr. Sci.* **2003**, *211* (2), 251−261.
(155) Saxena, A.; Tripathi, B. P.; Kumar, M.; Shahi, V. K. Membrane-based techniques for the separation and purification of proteins: An overview. *Adv. Colloid Interface Sci.* **2009**, *145* (1−2), 1−22.
(156) Lin, J.; Ye, W.; Huang, J.; Ricard, B.; Baltaru, M.-C.; Greydanus, B.; Balta, S.; Shen, J.; Vlad, M.; Sotto, A.; et al. Toward resource recovery from textile wastewater: dye extraction, water and base/acid regeneration using a hybrid NF-BMED process. *ACS Sustain. Chem. Eng.* **2015**, *3* (9), 1993−2001.
(157) Liu, R.; Arabale, G.; Kim, J.; Sun, K.; Lee, Y.; Ryu, C.; Lee, C. Graphene oxide membrane for liquid phase organic molecular separation. *Carbon* **2014**, *77*, 933−938.
(158) Sun, P.; Zheng, F.; Wang, K.; Zhong, M.; Wu, D.; Zhu, H. Electro-and magneto-modulated ion transport through graphene oxide membranes. *Sci. Rep.* **2014**, *4* (1), 1−9.
(159) Mehrabi, N.; Lin, H.; Aich, N. Deep eutectic solvent functionalized graphene oxide nanofiltration membranes with superior water permeance and dye desalination performance. *Chem. Eng. J.* **2021**, *412*, No. 128577.
(160) Liu, J.; Wang, N.; Yu, L.-J.; Karton, A.; Li, W.; Zhang, W.; Guo, F.; Hou, L.; Cheng, Q.; Jiang, L.; et al. Bioinspired graphene membrane with temperature tunable channels for water gating and molecular separation. *Nat. Commun.* **2017**, *8* (1), 2011.
(161) Zhang, W.-H.; Yin, M.-J.; Jin, C.-G.; Liu, Z.-J.; Wang, N.; An, Q.-F. Ice-crystal templating approach for tailoring mass transfer channels in graphene oxide membranes for high-performance dye/salt separation. *Carbon* **2021**, *183*, 119−127.
(162) Jacoby, M. It's time to recycle lithium-ion batteries. *Chem. Eng. News* **2019**, *97* (28), 29.
(163) Dang, H.; Li, N.; Chang, Z.; Wang, B.; Zhan, Y.; Wu, X.; Liu, W.; Ali, S.; Li, H.; Guo, J.; et al. Lithium leaching via calcium chloride roasting from simulated pyrometallurgical slag of spent lithium ion battery. *Sep. Purif. Technol.* **2020**, *233*, No. 116025.
(164) Makuza, B.; Tian, Q.; Guo, X.; Chattopadhyay, K.; Yu, D. Pyrometallurgical options for recycling spent lithium-ion batteries: A comprehensive review. *J. Power Sources* **2021**, *491*, No. 229622.
(165) Biswal, B. K.; Jadhav, U. U.; Madhaiyan, M.; Ji, L.; Yang, E.-H.; Cao, B. Biological leaching and chemical precipitation methods for recovery of Co and Li from spent lithium-ion batteries. *ACS Sustain. Chem. Eng.* **2018**, *6* (9), 12343−12352.
(166) Nan, J.; Han, D.; Zuo, X. Recovery of metal values from spent lithium-ion batteries with chemical deposition and solvent extraction. *J. Power Sources* **2005**, *152*, 278−284.
(167) Kumar, R.; Chakrabortty, S.; Chakrabortty, P.; Nayak, J.; Liu, C.; Khan, M. A.; Ha, G.-S.; Kim, K. H.; Son, M.; Roh, H.-S.; et al. Sustainable recovery of high-valued resources from spent lithium-ion batteries: A review of the membrane-integrated hybrid approach. *Chem. Eng. J.* **2023**, *470*, No. 144169.
(168) Xu, P.; Dai, Q.; Gao, H.; Liu, H.; Zhang, M.; Li, M.; Chen, Y.; An, K.; Meng, Y. S.; Liu, P.; et al. Efficient direct recycling of lithium-ion battery cathodes by targeted healing. *Joule* **2020**, *4* (12), 2609−2626.
(169) Kumar, R.; Liu, C.; Ha, G.-S.; Park, Y.-K.; Khan, M. A.; Jang, M.; Kim, S.-H.; Amin, M. A.; Gacem, A.; Jeon, B.-H.; et al. Downstream recovery of Li and value-added metals (Ni, Co, and Mn) from leach liquor of spent lithium-ion batteries using a membrane-integrated hybrid system. *Chem. Eng. J.* **2022**, *447*, No. 137507.
(170) Cheng, Q.; Wang, Z.; Wang, Y.; Li, J.-T.; Fu, H. Recent advances in preferentially selective Li recovery from spent lithium-ion batteries: A review. *J. Environ. Chem. Eng.* **2024**, *12*, No. 112903.
(171) Cao, Y.; Luo, J.; Chen, C.; Wan, Y. Highly permeable acid-resistant nanofiltration membrane based on a novel sulfonamide aqueous monomer for efficient acidic wastewater treatment. *Chem. Eng. J.* **2021**, *425*, No. 131791.
(172) Wang, L.; Guo, X.; Cao, K.; Li, B.; Li, Y.; Zhang, M.; Wen, R.; Li, X.; Li, S.; Ma, L. Effective charge-discriminated group separation of metal ions under highly acidic conditions using nanodiamond-pillared graphene oxide membrane. *J. Mater. Chem. A* **2017**, *5* (17), 8051−8061.
(173) Li, X.; Mo, Y.; Qing, W.; Shao, S.; Tang, C. Y.; Li, J. Membrane-based technologies for lithium recovery from water lithium resources: A review. *J. Membr. Sci.* **2019**, *591*, No. 117317.
(174) Xi, Y.-H.; Liu, Z.; Ji, J.; Wang, Y.; Faraj, Y.; Zhu, Y.; Xie, R.; Ju, X.-J.; Wang, W.; Lu, X.; et al. Graphene-based membranes with uniform 2D nanochannels for precise sieving of mono-/multi-valent metal ions. *J. Membr. Sci.* **2018**, *550*, 208−218.
(175) Liang, S.; Wang, S.; Chen, L.; Fang, H. Controlling interlayer spacings of graphene oxide membranes with cationic for precise sieving of mono-/multi-valent ions. *Sep. Purif. Technol.* **2020**, *241*, No. 116738.
(176) Rahighi, R.; Hosseini-Hosseinabad, S. M.; Zeraati, A. S.; Suwaileh, W.; Norouzi, A.; Panahi, M.; Gholipour, S.; Karaman, C.; Akhavan, O.; Khollari, M. A. R.; et al. Two-dimensional materials in enhancement of membrane-based lithium recovery from metallic-ions-rich wastewaters: A review. *Desalination* **2022**, *543*, No. 116096.
(177) Wu, T.; Wang, Z.; Lu, Y.; Liu, S.; Li, H.; Ye, G.; Chen, J. Graphene oxide membranes for tunable ion sieving in acidic radioactive waste. *Advanced Science* **2021**, *8* (7), No. 2002717.
(178) Chen, Y.; Qiao, Q.; Cao, J.; Li, H.; Bian, Z. Precious metal recovery. *Joule* **2021**, *5* (12), 3097−3115.
(179) Chen, Y.; Xu, M.; Wen, J.; Wan, Y.; Zhao, Q.; Cao, X.; Ding, Y.; Wang, Z. L.; Li, H.; Bian, Z. Selective recovery of precious metals through photocatalysis. *Nat. Sustain.* **2021**, *4* (7), 618−626.
(180) Yang, S.; Zhang, F.; Ding, H.; He, P.; Zhou, H. Lithium metal extraction from seawater. *Joule* **2018**, *2* (9), 1648−1651.
(181) Lim, Y. J.; Goh, K.; Goto, A.; Zhao, Y.; Wang, R. Uranium and lithium extraction from seawater: challenges and opportunities for a sustainable energy future. *J. Mater. Chem. A* **2023**, *11*, 22551−22589.
(182) Kim, N.; Su, X.; Kim, C. Electrochemical lithium recovery system through the simultaneous lithium enrichment via sustainable redox reaction. *Chem. Eng. J.* **2021**, *420*, No. 127715.
(183) Battistel, A.; Palagonia, M. S.; Brogioli, D.; La Mantia, F.; Trócoli, R. Electrochemical methods for lithium recovery: a comprehensive and critical review. *Adv. Mater.* **2020**, *32* (23), No. 1905440.
(184) Mends, E. A.; Chu, P. Lithium extraction from unconventional aqueous resources−a review on recent technological development for seawater and geothermal brines. *J. Environ. Chem. Eng.* **2023**, *11* (5), No. 110710.
(185) Lundaev, V.; Solomon, A.; Caldera, U.; Breyer, C. Material extraction potential of desalination brines: A technical and economic evaluation of brines as a possible new material source. *Miner. Eng.* **2022**, *185*, No. 107652.
(186) Zhang, M.; Zhao, P.; Li, P.; Ji, Y.; Liu, G.; Jin, W. Designing biomimic two-dimensional ionic transport channels for efficient ion sieving. *ACS Nano* **2021**, *15* (3), 5209−5220.
(187) Zhang, W.; Huang, Q.; Liu, S.; Zhang, M.; Liu, G.; Ma, Z.; Jin, W. Graphene oxide membrane regulated by surface charges and interlayer channels for selective transport of monovalent ions over divalent ions. *Sep. Purif. Technol.* **2022**, *291*, No. 120938.
(188) Liu, S.; Tong, X.; Huang, L.; Xiao, C.; Zhang, K.; Chen, Y.; Crittenden, J. Lithium-ion extraction using electro-driven freestanding graphene oxide composite membranes. *J. Membr. Sci.* **2023**, *672*, No. 121448.

(189) Lipnizki, F.; Hausmanns, S.; Ten, P.-K.; Field, R. W.; Laufenberg, G. Organophilic pervaporation: prospects and performance. *Chem. Eng. J.* **1999**, *73* (2), 113−129.
(190) Al-Harby, N. F.; El Batouti, M.; Elewa, M. M. A Comparative Analysis of Pervaporation and Membrane Distillation Techniques for Desalination Utilising the Sweeping Air Methodology with Novel and Economical Pervaporation Membranes. *Polymers* **2023**, *15* (21), 4237.
(191) Aptel, P.; Challard, N.; Cuny, J.; Neel, J. Application of the pervaporation process to separate azeotropic mixtures. *J. Membr. Sci.* **1976**, *1*, 271−287.
(192) Nguyen, T. Q.; Nobe, K. Extraction of organic contaminants in aqueous solutions by pervaporation. *J. Membr. Sci.* **1987**, *30* (1), 11−22.
(193) Qian, X.; Li, N.; Wang, Q.; Ji, S. Chitosan/graphene oxide mixed matrix membrane with enhanced water permeability for high-salinity water desalination by pervaporation. *Desalination* **2018**, *438*, 83−96.
(194) Zhao, J.; Zhu, Y.; Pan, F.; He, G.; Fang, C.; Cao, K.; Xing, R.; Jiang, Z. Fabricating graphene oxide-based ultrathin hybrid membrane for pervaporation dehydration via layer-by-layer self-assembly driven by multiple interactions. *J. Membr. Sci.* **2015**, *487*, 162−172.
(195) Chen, X.; Mohammed, S.; Yang, G.; Qian, T.; Chen, Y.; Ma, H.; Xie, Z.; Zhang, X.; Simon, G. P.; Wang, H. Selective permeation of water through angstrom-channel graphene membranes for bioethanol concentration. *Adv. Mater.* **2020**, *32* (33), No. 2002320.
(196) Zhang, W.; Jia, J.; Qiu, Y.; Pan, K. Polydopamine-grafted graphene oxide composite membranes with adjustable nanochannels and separation performance. *Adv. Mater. Interfaces* **2018**, *5* (8), No. 1701386.
(197) Qian, Y.; Zhang, X.; Liu, C.; Zhou, C.; Huang, A. Tuning interlayer spacing of graphene oxide membranes with enhanced desalination performance. *Desalination* **2019**, *460*, 56−63.
(198) Zhang, X.; Zhang, M.-X.; Ding, H.; Yang, H.; Ma, X.-H.; Xu, X.-R.; Xu, Z.-L.; Tang, C. Y. Double-crosslinked GO interlayer framework as a pervaporation hybrid membrane with high performance. *ACS omega* **2019**, *4* (12), 15043−15050.
(199) Castro-Muñoz, R.; Buera-González, J.; de la Iglesia, O.; Galiano, F.; Fíla, V.; Malankowska, M.; Rubio, C.; Figoli, A.; Téllez, C.; Coronas, J. Towards the dehydration of ethanol using pervaporation cross-linked poly (vinyl alcohol)/graphene oxide membranes. *J. Membr. Sci.* **2019**, *582*, 423−434.
(200) Liu, G.; Jin, W. Pervaporation membrane materials: Recent trends and perspectives. *J. Membr. Sci.* **2021**, *636*, No. 119557.
(201) Huang, K.; Liu, G.; Shen, J.; Chu, Z.; Zhou, H.; Gu, X.; Jin, W.; Xu, N. High-efficiency water-transport channels using the synergistic effect of a hydrophilic polymer and graphene oxide laminates. *Adv. Funct. Mater.* **2015**, *25* (36), 5809−5815.
(202) Dai, L.; Xu, F.; Huang, K.; Xia, Y.; Wang, Y.; Qu, K.; Xin, L.; Zhang, D.; Xiong, Z.; Wu, Y.; et al. Ultrafast water transport in two-dimensional channels enabled by spherical polyelectrolyte brushes with controllable flexibility. *Angew. Chem.* **2021**, *133* (36), 20086−20094.
(203) Yang, G.; Xie, Z.; Cran, M.; Ng, D.; Easton, C. D.; Ding, M.; Xu, H.; Gray, S. Functionalizing graphene oxide framework membranes with sulfonic acid groups for superior aqueous mixture separation. *J. Mater. Chem. A* **2019**, *7* (34), 19682−19690.
(204) Liu, Q.; Wu, Y.; Wang, X.; Liu, G.; Zhu, Y.; Tu, Y.; Lu, X.; Jin, W. Molecular dynamics simulation of water-ethanol separation through monolayer graphene oxide membranes: Significant role of O/C ratio and pore size. *Sep. Purif. Technol.* **2019**, *224*, 219−226.
(205) Foller, T.; Madauß, L.; Ji, D.; Ren, X.; De Silva, K. K. H.; Musso, T.; Yoshimura, M.; Lebius, H.; Benyagoub, A.; Kumar, P. V.; et al. Mass transport via in-plane nanopores in graphene oxide membranes. *Nano Lett.* **2022**, *22* (12), 4941−4948.
(206) El-Bourawi, M.; Ding, Z.; Ma, R.; Khayet, M. A framework for better understanding membrane distillation separation process. *J. Membr. Sci.* **2006**, *285* (1−2), 4−29.
(207) Alklaibi, A. M.; Lior, N. Membrane-distillation desalination: status and potential. *Desalination* **2005**, *171* (2), 111−131.
(208) Subrahmanya, T.; Austria, H. F. M.; Chen, Y.-Y.; Setiawan, O.; Widakdo, J.; Kurkuri, M. D.; Hung, W.-S.; Hu, C.-C.; Lee, K.-R.; Lai, J.-Y. Self-surface heating membrane distillation for sustainable production of freshwater: A state of the art overview. *Prog. Mater. Sci.* **2024**, *145*, No. 101309.
(209) Choi, Y.; Naidu, G.; Nghiem, L. D.; Lee, S.; Vigneswaran, S. Membrane distillation crystallization for brine mining and zero liquid discharge: opportunities, challenges, and recent progress. *Environ. Sci.: Water Res. Technol.* **2019**, *5* (7), 1202−1221.
(210) Eryildiz, B.; Ozbey-Unal, B.; Gezmis-Yavuz, E.; Koseoglu-Imer, D. Y.; Keskinler, B.; Koyuncu, I. Flux-enhanced reduced graphene oxide (rGO)/PVDF nanofibrous membrane distillation membranes for the removal of boron from geothermal water. *Sep. Purif. Technol.* **2021**, *274*, No. 119058.
(211) Bhadra, M.; Roy, S.; Mitra, S. Desalination across a graphene oxide membrane via direct contact membrane distillation. *Desalination* **2016**, *378*, 37−43.
(212) Xu, Z.; Yan, X.; Du, Z.; Li, J.; Cheng, F. Effect of oxygenic groups on desalination performance improvement of graphene oxide-based membrane in membrane distillation. *Sep. Purif. Technol.* **2020**, *251*, No. 117304.
(213) Seo, D. H.; Pineda, S.; Woo, Y. C.; Xie, M.; Murdock, A. T.; Ang, E. Y.; Jiao, Y.; Park, M. J.; Lim, S. I.; Lawn, M.; et al. Anti-fouling graphene-based membranes for effective water desalination. *Nat. Commun.* **2018**, *9* (1), 683.
(214) Seraj, S.; Mohammadi, T.; Tofighy, M. A. Graphene-based membranes for membrane distillation applications: A review. *J. Environ. Chem. Eng.* **2022**, *10* (3), No. 107974.
(215) Lou, M.; Huang, S.; Zhu, X.; Chen, J.; Fang, X.; Li, F. Dual-polymers inserted graphene oxide membranes with enhanced anti-wetting and anti-scaling performance for membrane distillation. *J. Membr. Sci.* **2024**, *697*, No. 122494.
(216) Chen, H.; Mao, Y.; Mo, B.; Pan, Y.; Xu, R.; Ji, W.; Chen, G.; Liu, G.; Jin, W. Plasma-assisted facile fabrication of omniphobic graphene oxide membrane with anti-wetting property for membrane distillation. *J. Membr. Sci.* **2023**, *668*, No. 121207.
(217) Baker, R. W. *Membrane Technology and Applications*; John Wiley & Sons, 2012.
(218) Goon, G. S.S.; Labban, O.; Foo, Z. H.; Zhao, X.; Lienhard, J. H. Deformation-induced cleaning of organically fouled membranes: Fundamentals and techno-economic assessment for spiral-wound membranes. *J. Membr. Sci.* **2021**, *626*, No. 119169.
(219) Drioli, E.; Giorno, L. *Encyclopedia of membranes*; Springer Berlin: Heidelberg, Berlin, 2016.
(220) Togo, N.; Nakagawa, K.; Shintani, T.; Yoshioka, T.; Takahashi, T.; Kamio, E.; Matsuyama, H. Osmotically assisted reverse osmosis utilizing hollow fiber membrane module for concentration process. *Ind. Eng. Chem. Res.* **2019**, *58* (16), 6721−6729.
(221) Qasim, M.; Badrelzaman, M.; Darwish, N. N.; Darwish, N. A.; Hilal, N. Reverse osmosis desalination: A state-of-the-art review. *Desalination* **2019**, *459*, 59−104.
(222) Liu, H.; Huang, X.; Wang, Y.; Kuang, B.; Li, W. Nanowire-assisted electrochemical perforation of graphene oxide nanosheets for molecular separation. *Nat. Commun.* **2024**, *15* (1), 164.
(223) Saraswat, V.; Jacobberger, R. M.; Ostrander, J. S.; Hummell, C. L.; Way, A. J.; Wang, J.; Zanni, M. T.; Arnold, M. S. Invariance of water permeance through size-differentiated graphene oxide laminates. *ACS Nano* **2018**, *12* (8), 7855−7865.
(224) Peng, L. E.; Yang, Z.; Long, L.; Zhou, S.; Guo, H.; Tang, C. Y. A critical review on porous substrates of TFC polyamide membranes: Mechanisms, membrane performances, and future perspectives. *J. Membr. Sci.* **2022**, *641*, No. 119871.
(225) Nam, Y. T.; Kim, S. J.; Kang, K. M.; Jung, W.-B.; Kim, D. W.; Jung, H.-T. Enhanced nanofiltration performance of graphene-based membranes on wrinkled polymer supports. *Carbon* **2019**, *148*, 370−377.
(226) Zhang, M.; Sun, J.; Mao, Y.; Liu, G.; Jin, W. Effect of substrate on formation and nanofiltration performance of graphene oxide membranes. *J. Membr. Sci.* **2019**, *574*, 196−204.

(227) Wu, C.; Long, L.; Yang, Z.; Tang, C. Y. Porous substrate affects fouling propensity of thin-film composite nanofiltration membranes. *J. Membr. Sci. Lett.* **2022**, *2* (2), No. 100036.
(228) Zhang, M.; Mao, Y.; Liu, G.; Liu, G.; Fan, Y.; Jin, W. Molecular bridges stabilize graphene oxide membranes in water. *Angew. Chem.-Int. Ed.* **2020**, *59* (4), 1689−1695.
(229) Enfrin, M.; Lee, J.; Le-Clech, P.; Dumée, L. F. Kinetic and mechanistic aspects of ultrafiltration membrane fouling by nano-and microplastics. *J. Membr. Sci.* **2020**, *601*, No. 117890.
(230) Xiao, T.; Zhu, Z.; Li, L.; Shi, J.; Li, Z.; Zuo, X. Membrane fouling and cleaning strategies in microfiltration/ultrafiltration and dynamic membrane. *Sep. Purif. Technol.* **2023**, *318*, No. 123977.
(231) Shahzad, A.; Oh, J.-M.; Azam, M.; Iqbal, J.; Hussain, S.; Miran, W.; Rasool, K. Advances in the synthesis and application of anti-fouling membranes using two-dimensional nanomaterials. *Membranes* **2021**, *11* (8), 605.
(232) Sun, J.; Hu, C.; Liu, Z.; Liu, H.; Qu, J. Surface charge and hydrophilicity improvement of graphene membranes via modification of pore surface oxygen-containing groups to enhance permeability and selectivity. *Carbon* **2019**, *145*, 140−148.
(233) Tian, L.; Zhou, P.; Graham, N.; Li, G.; Yu, W. Long-term operation and biofouling of graphene oxide membrane in practical water treatment: Insights from performance and biofilm characteristics. *J. Membr. Sci.* **2023**, *680*, No. 121761.
(234) Abebe, S. H.; Subrahmanya, T.; Austria, H. F. M.; Nayak, S.; Huang, T.-H.; Setiawan, O.; Hung, W.-S.; Hu, C.-C.; Lee, K.-R.; Lai, J.-Y. High performance lamellar structured graphene oxide nanocomposite membranes via Fe3O4-coordinated phytic acid control of interlayer spacing for organic solvent nanofiltration (OSN). *Chem. Eng. J.* **2024**, *495*, No. 153451.
(235) Hoek, E. M.; Elimelech, M. Cake-enhanced concentration polarization: a new fouling mechanism for salt-rejecting membranes. *Environ. Sci. Technol.* **2003**, *37* (24), 5581−5588.
(236) Bai, W.; Samineni, L.; Chirontoni, P.; Krupa, I.; Kasak, P.; Popelka, A.; Saleh, N. B.; Kumar, M. Quantifying and reducing concentration polarization in reverse osmosis systems. *Desalination* **2023**, *554*, No. 116480.
(237) Chong, J. Y.; Wang, B.; Mattevi, C.; Li, K. Dynamic microstructure of graphene oxide membranes and the permeation flux. *J. Membr. Sci.* **2018**, *549*, 385−392.